Universidade de Aveiro
Ano 2013

Departamento de Electrónica, Telecomunicações e Informática

Tiago José Alves Marques

Esquemas de Cooperação entre Estações Base para o LTE no *Downlink*

Cooperation Schemes between Base Stations for LTE on the Downlink

Universidade de Aveiro
Ano 2013

Departamento de Electrónica, Telecomunicações e Informática

Tiago José Alves Marques

Esquemas de Cooperação entre Estações Base para o LTE no Sentido Descendente

Cooperation Schemes between Base Stations for LTE on the Downlink

Dissertação apresentada à Universidade de Aveiro para cumprimento dos requisitos necessários à obtenção do grau de Mestre em Engenharia Electrónica e Telecomunicações, realizada sob a orientação científica do Prof. Dr. Adão Paulo Soares da Silva, Departamento de Electrónica, Telecomunicações e Informática, Universidade de Aveiro; e do Prof. Dr. Atílio Manuel da Silva Gameiro, Departamento de Electrónica, Telcomunicações e Informática, Universidade de Aveiro.

o júri / the jury

presidente / president	**Prof. Dr. José Rodrigues Ferreira da Rocha** Professor Catedrático do Departamento de Electrónica, Telecomunicações e Informática da Universidade de Aveiro
orientador / adviser	**Prof. Dr. Adão Paulo Soares da Silva** Professor Auxiliar do Departamento de Electrónica, Telecomunicações e Informática da Universidade de Aveiro
co-orientador / co-adviser	**Prof. Dr. Atílio Manuel da Silva Gameiro** Professor Auxiliar do Departamento de Electrónica, Telecomunicações e Informática da Universidade de Aveiro
arguente / examiner	**Prof. Dr. Paulo Jorge Coelho Marques** Professor Adjunto do Instituto Politécnico de Castelo Branco

agradecimentos / acknowledgements

No momento em que findo o meu percurso académico, é com especial contentamento que agradeço a todas as pessoas que de certo modo me apoiaram ao longo deste curso, e sem os quais nada disto seria possível.

Primeiramente, gostaria de agradecer aos meus pais e restante família, por me permitirem enveredar neste percurso académico, e sempre acreditarem nas minhas capacidades.

À Universidade de Aveiro, principalmente ao Departamento de Engenharia Electrónica e Telecomunicações e ao Instituto de Telecomunicações, por me fornecerem os meios necessários à realização, não só desta dissertação, mas também do curso em si.

Ao Prof. Adão Silva, pela exímia orientação ao longo desta dissertação, pela oportunidade que me concedeu de poder realizar este trabalho e pela transmissão de conhecimentos ao longo deste ano.

A todos os meus amigos e colegas pelo espírito de camaradagem, amizade e entreajuda neste percurso académico.

E finalmente à Cândida, por sempre acreditar em mim e ser a minha maior motivação.

A todos, um bem-haja!

palavras-chave LTE, COMP, LTE-Advanced, OFDM, MIMO, DZF, DVSINR.

resumo

O crescimento exponencial no tráfego de comunicações sem-fios e no número de dispositivos utilizados (smart phones, computadores portáteis, etc.) está a causar um aumento significativo nos níveis de interferência, que prejudicam significativamente os ganhos de capacidade assegurados pelas tecnologias baseadas em ligações ponto-a-ponto MIMO. Deste modo, torna-se cada vez mais necessário que os grandes aperfeiçoamentos na eficiência espectral de sistemas de comunicações sem-fios tenham em consideração a interferência entre células. De forma a tomar em consideração estes aspectos, uma nova arquitectura celular terá de ser desenvolvida. É assim, neste contexto, que surge o LTE-Advanced.

Uma das tecnologias mais promissoras do LTE-*Advanced* é a Coordenação Multi-Ponto (CoMP), que permite que as estações base cooperem de modo a mitigar a interferência entre células e, deste modo, aumentar a capacidade do sistema. Esta dissertação pretende estudar este conceito, implementando para isso algumas técnicas que se enquadram no conceito do CoMP.

Nesta dissertação iremos considerar a implementação de um sistema de pré-codificação em múltiplas células, em que os pré-codificadores são calculados em cada BS, de modo a mitigar a interferência entre células. São considerados dois pré-codificadores: *Distributed Zero Forcing* (DZF) e *Distributed Virtual Signal-to-Interferance Noise Ratio* (DVSINR), recentemente proposto. De seguida o sistema é optimizado com a introdução de algoritmos de alocação de potência entre as sub-portadoras com o objectivo de minimizar a taxa média de erros (BER). Os algoritmos considerados são também avaliados em situações em que a informação do estado do canal é imperfeita. Uma versão quantizada da CSI associada a cada uma das diferentes ligações entre as BS e os UT é assim enviada do UT para a BS. Esta informação é então utilizada para calcular os diferentes pré-codificadores em cada BS. Uma nova versão do pré-codificador DVSINR é proposta de modo a lidar com CSI imperfeito.

Os esquemas propostos foram implementados considerandos especificações do LTE, e os resultados obtidos demonstram que os pré-codificadores removem de uma forma eficiente a interferência, mesmo em situações em que a CSI é imperfeita.

key-words LTE, COMP, LTE-Advanced, OFDM, MIMO, DZF, DVSINR.

abstract

The explosive growth in wireless traffic and in the number of connected devices as smart phones or computers, are causing a dramatic increase in the levels of interference, which significantly degrades the capacity gains promised by the point-to-point multi input, multi output (MIMO) based techniques. Therefore, it is becoming increasingly clear that major new improvements in spectral efficiency of wireless networks will have to entail addressing intercell interference. So, there is a need for a new cellular architecture that can take these factors under consideration. It is in this context that LTE-Advanced arises.

One of the most promising LTE-Advanced technology is Coordinated Multipoint (CoMP), which allows base stations to cooperate among them, in order to mitigate or eliminate the intercell interference and, by doing so, increase the system's capacity. This thesis intends to study this concept, implementing some schemes that fall under the CoMP concept.

In this thesis we consider a distributed precoded multicell approach, where the precoders are computed locally at each BS to mitigate the intercell interference. Two precoder are considered: distributed zero forcing (DZF) and distributed virtual signal-to-interference noise ratio (DVSINR) recently proposed. Then the system is further optimized by computing a power allocation algorithm over the subcarriers that minimizes the average bit error rate (BER). The considered algorithms are also evaluated under imperfect channel state information. A quantized version of the CSI associated to the different links between the BS and the UT is feedback from the UT to the BS. This information is then employed by the different BSs to perform the precoding design. A new DVSINR precoder explicitly designed under imperfect CSI is proposed.

The proposed schemes were implemented considering the LTE specifications, and the results show that the considered precoders are efficiently to remove the interference even under imperfect CSI.

Table of Contents

List of Figures

List of Tables

Acronyms

1G	First Generation
2G	Second Generation
3G	Third Generation
3GPP	3rd Generation Partnership Project
4G	Fourth Generation
AES	Advanced Encryption Standard
ARQ	Automatic Repeat Request
AWGN	Additive White Gaussian Noise
BD	Block Diagonalization
BER	Bit Error Rate
BS	Base Station
CAPEX	Capital Expendables
CB	Coordinated Beamforming
CCs	Component Carriers
CDMA	Code Division Multiple Access
CIR	Channel Impulse Response
CJP	Centralized Joint Processing
CM	Cubic Metric
CoMP	Coordinated Multipoint
CP	Cyclic Prefix
CRC	Cyclic Redundancy Check
CS	Coordinated Scheduling
CSI	Channel State Information
CU	Central Unit
DFT-S-OFDM	Discrete Fourier transform spread OFDM
DJP	Distributed Joint Processing
DoF	Degrees of Freedom
DVSINR	Distributed Virtual Signal-to-Interference Noise Ratio
DwPTS	Downlink Pilot Timeslot
DZF	Distributed Zero Forcing
EAP	Extensible Authentication Protocol
EGC	Equal Gain Combining
eNB	evolved Node-B
EPC	Evolved Packet Core
EPS	Evolved Packet System
E-UTRAN	Evolved UMTS Terrestrial Radio Access Network
FDMA	Frequency Division Multiple Access

FEC	Forward Error Correction
FFT	Fast Fourier Transform
GP	Guard Period
GPRS	General Packet Radio Service
GSM	Global System for Mobile communications
HARQ	Hybrid Automatic Repeat Request
HRPD	High Rate Packet Data
HSPA	High Speed Packet Access
HSS	Home Subscriber Server
ICI	Inter-Carrier Interference
ICIN	Inter-Cell Interference Nulling
IFFT	Inverse Fourier Transform
IMS	IP Multimedia Subsystem
IMT-2000	International Mobile Telecommunications 2000
IP	Internet Protocol
IS-95	Interim Standard 95
ISI	Inter-Symbolic Interference
ITU-R	International Telecommunication Union - Radiocommunication Sector
JLS	Joint Leakage Suppression
JP	Joint Processing
JT	Joint Transmission
KKT	Karush-Kuhn-Tucker
LTE	Long-Term Evolution
MAC	Media Access Control layer
MIMO	Multiple Input Multiple Output
MISO	Multiple Input Multiple Output
MME/GW	Mobility Management Entity/Gateway
MMSEC	Minimum Mean Square Error Combining
MRC	Maximum Ratio Combining
MT	Mobile Termination
MU-MIMO	Multi-user MIMO
OFDM	Orthogonal Frequency Division Multiplexing
OFDMA	Orthogonal Frequency-Division Multiple Access
OPEX	Operational Expendables
PAPR	Peak-to-Average Power Ratio
PBCH	Physical broadcast channel
PCCC	Parallel Concatenated Convolutional Code
PCFICH	Physical Control Format Indicator Channel
PCFICH	Physical Control Format Indicator Channel
PDCCH	Physical Downlink Control Channel

PDCP	Packet Data Convergence Protocol
PDN	Packet Data Network
PDP	Power Delay Profile
PDSCH	Physical Downlink Shared Channel
P-GW	PDN gateway
PHICH	Physical HARQ Indicator Channel
PHY	Physical layer
PJP	Partial Joint Processing
PLMN	Public Land Mobile Network
PMI	Precoding Matrix Indicator
PRACH	Physical Random Access Channel
PUCCH	Physical Uplink Control Channel
QAM	Quadrature Amplitude Modulation
QoS	Quality of Service
QPSK	Quadrature Phase-Shift Keying
RB	Resource Blocks
R-DVSINR	Robust-DVSINR
RE	Resource Element
RLC	Radio Link Control
RN	Relay Nodes
RNC	Radio Network Controller
SAE	System Architecture Evolution
SC	Single Carrier
SC-FDMA	Single Carrier Frequency Domain Multiple Access
SDMA	Space Division Multiple Access
SFBC	Space-Frequency Block Coding
S-GW	Serving Gateway
SIMO	Single Input Multiple Output
SISO	Single-input single-output
SLNR	Signal-to-Leakage-plus-Noise Ratio
SNR	Signal-to-Noise Ratio
SON	Self-Organization Network
STBC	Space-Time Block Coding
TDD	Time Division Duplexing
TDMA	Time Division Multiple Access
TD-SCDMA	Time Division Synchronous Code Division Multiple Access
TE	Terminal Equipment
TFST	Time-Frequency Synchronization Transmission
TP	Transmission Point
UMB	Ultra Mobile Broadband

UMTS	Universal Telecommunications System
UpPTS	Uplink Pilot Timeslot
UT	User Terminal
VoIP	Voice over Internet Protocol
WCDMA	Wideband CDMA
WiMAX	Worldwide Interoperability for Microwave Access
ZF	Zero Forcing
ZFBF	Zero-Forcing Beamforming
ZFC	Zero Forcing Combining

1. Introduction

1.1. Cellular Communications Evolution

In the past decades, the wireless communications industry has witnessed a tremendous growth, with over six billion wireless subscribers worldwide [1]. The first generation (1G) of cellular communication systems was analog and only supported voice communications with limited roaming. The individual cells were large and the system did not use the available radio spectrum efficiently, so their capacity was very small. The mobile devices were very large and expensive, and had a very restricted users circle.

The second generation (2G) marked the turn of cellular communications to digital systems. This change came with a promise of higher capacity and better voice quality than their analog counterparts. This permitted a more efficient use of the radio spectrum and the introduction of cheaper and smaller mobile devices.

The two widely deployed second generation (2G) systems are the Time Division Multiple Access (TDMA) based GSM (Global System for Mobile communications) and CDMA (Code Division Multiple Access) based Interim Standard 95 (IS-95). These 2G systems were designed to support voice communications, but later on, there were introduced capabilities to support data transmissions. This new systems, called 2.5G, introduced a core network's packet switched domain and a modified air interface. The *General Packet Radio Service* (GPRS), a best-effort service that used packet switching data transmissions and could provide data rates from 56 up to 114kbps, incorporated these techniques into GSM. However, data rates of these transmissions were generally lower than that supported by dial-up connections [2].

The ITU-R initiative on IMT-2000 (International Mobile Telecommunications 2000) paved the way to evolution to 3G systems, setting requirements such as a peak data rate of 2Mbits/s and support for vehicular mobility [3]. Both the GSM and CDMA camps formed their own separate 3G partnerships (3GPP and 3GPP2, respectively) to develop IMT-2000 compliant standard, based on CDMA technology. The 3G standard in the 3GPP group is called wideband CDMA (WCDMA) because of its use of a larger 5MHz bandwidth, relatively to a 1.25MHz bandwidth used in 3GPP2's cdma2000 system.

The world's dominant 3G system is called Universal Telecommunications System (UMTS) and it encloses the WCDMA system, the most used in the world, as well as Time Division Synchronous Code Division Multiple Access (TD-SCDMA), a derivative of WCDMA, which is also known as the low chip rate option of UMTS TDD (Time Division Duplex) mode [4]. This later is mostly

used in China. While WCDMA segregates the base stations' and mobiles' transmissions by means of frequency division duplex (FDD), TD-SCDMA uses TDD, and also a smaller carrier of 1.6MHz.

The first release of the 3G standard did not fulfill its promise of high-speed data transmissions as the data rates supported in practice were much lower than that claimed in the standards. In order to enhance the 3G system for efficient data support, 3GPP2 introduced the HRPD (High Rate Packet Data, also called cdma2000-1xEVDO – evolution data only) system, which uses techniques such as channel sensitive scheduling, fast link adaptation and hybrid ARQ, to optimize the data traffic. This system required a separate 1.25MHz carrier and did not support voice traffic. The 3GPP group introduced the HSPA (High Speed Packet Access) enhancement to the WCDMA system. It reused many of the same data-optimized techniques as the HRPD, but it could have both voice and data services in the same 5MHz carrier, by code-multiplexing them. In the later version of HRPD, VoIP (Voice over Internet Protocol) capabilities were introduced to provide both voice and data services on the same carrier.

While HSPA and HRPD were being developed and deployed, IEEE 802 LMSC (LAN/MAN Standard Committee) introduced the IEEE 802.16e standard form mobile broadband wireless access, which has been commercialized under the Worldwide Interoperability for Microwave Access (WiMAX) label by the WiMAX Forum. The mobile version of the standard IEEE 802.16e is referred as Mobile WiMAX and employed a different access technology named OFDMA (Orthogonal Frequency Division Multiple Access) and claimed better data rates and spectral efficiency than that provided by HSPA and HRPD.

The main features of Mobile WiMAX also includes MIMO techniques, scalability from different channels (from 1.25 to 20 MHz), improved security with Extensible Authentication Protocol (EAP) based authentication and Advanced Encryption Standard (AES) based authentication encryption and optimized handover schemes with latencies lower than 50 milliseconds [5].

The introduction of Mobile WiMAX led both 3GPP and 3GPP2 to develop their own version of beyond 3G systems based on the OFDMA technology and network architecture similar to that in Mobile WiMAX. The beyond 3G systems in 3GPP is called evolved universal terrestrial radio access (evolved UTRA) and is also widely referred to as LTE (Long-Term Evolution) while 3GPP2's version is called UMB (Ultra Mobile Broadband).In November 2008, Qualcomm, UMB's lead sponsor, announced it was ending development of the technology, favoring LTE instead [6].

Using OFDMA and MIMO based technology, LTE provides peak data rates of 300Mbps in the downlink and 75Mbps in the uplink, as well as QoS provisions that allows the system to transfer with a latency of less than 5ms in the radio access network. It enables the possibility of managing fast-moving mobiles and to support multi-cast and broadcast streams. One of the major changes, compared to its precedents systems, is the introduction of an IP-based network architecture, called Evolved Packet Core (EPC). This network architecture was designed to replace the GPRS core network and supports seamless handovers for both voice and data cell towers, with older technology, such as GSM, UMTS or CDMA2000. LTE will be further discussed in Chapter 4.

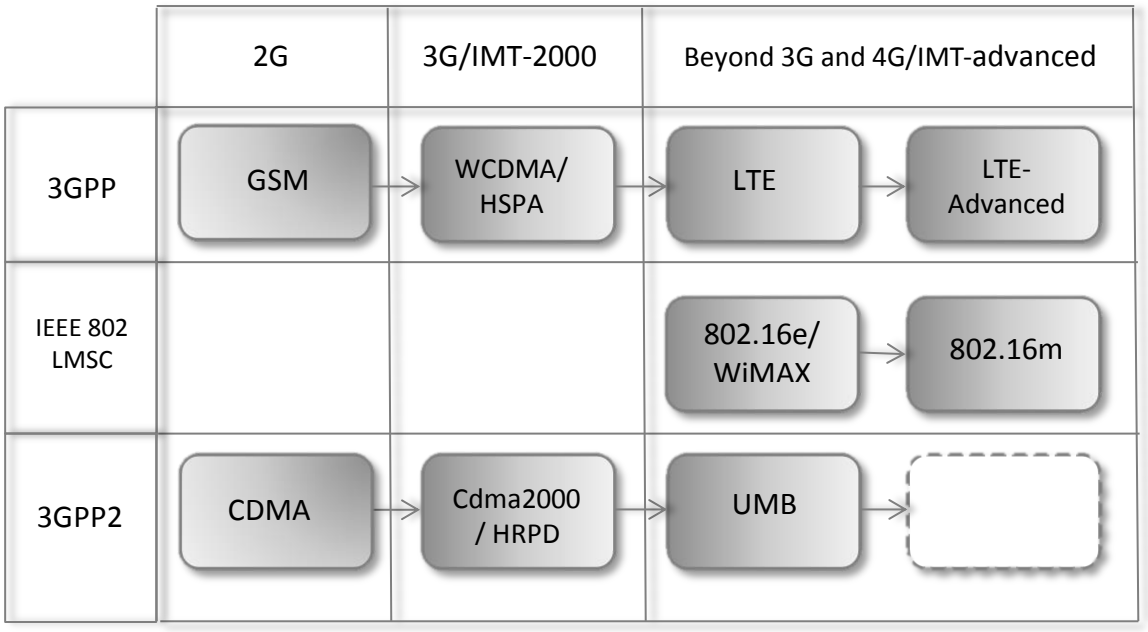

Figure 1 - Cellular Systems Evolution

In the first quarter of 2013 6.5 billion cellular connections were registered, as we can see in the figure bellow. From this, 90% are still GSM – HSPA users, and only 1.4% are from LTE users, but the number is increasing, seen as in the fourth quarter of 2012 only 68 Million users were registered [7].

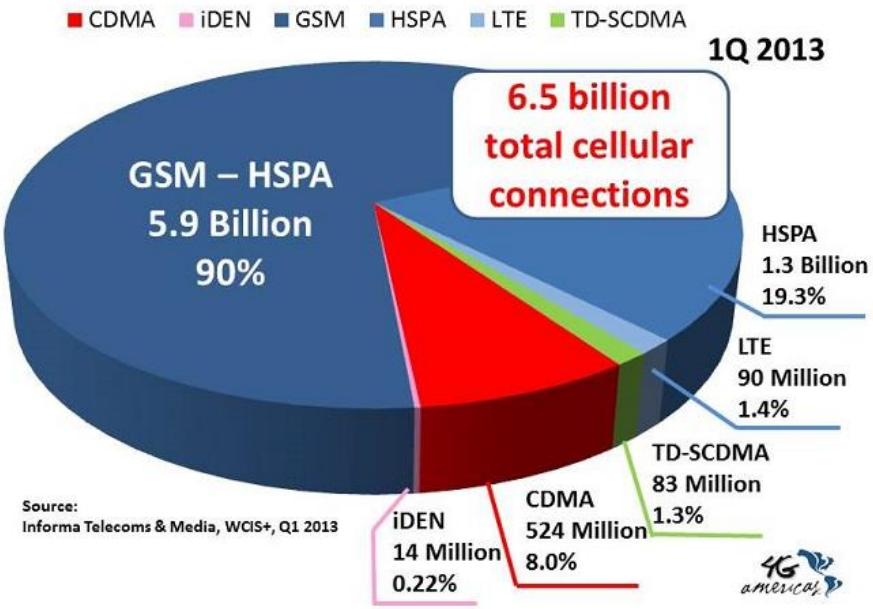

Figure 2 - Subscriptions of Cellular Systems [7]

1.2. Motivation and Objectives

4G cellular systems, designated by LTE have recently been deployed, allowing transmission rates way above those seen in 3G systems. However, the increasing demand for higher transmission rate systems cannot be fulfilled by the current cellular architecture. In cellular systems, a way to increase transmission rates is to decrease the cells size, decreasing then the path loss. Nonetheless, considering the current cellular architecture and the unitary frequency reuse, that would lead to a huge increase of users' interference in the cells edge, leading to a considerable degradation of the systems performance.

In this context it is necessary to develop new cellular architectures that can allow us to reduce or even eliminate interference between the users' terminals (UTs), mainly at the cell edges. Multicell cooperation or coordination is a promising solution for cellular wireless systems to mitigate intercell interference, improving system fairness and increasing capacity, and thus is already under study in LTE-Advanced under the coordinated multipoint (CoMP) concept.

There are several multicell based approaches depending on the amount of information shared by the base stations (BSs) through the backhaul network and where the processing takes place, i.e., centralized if the processing takes place at the central unit (CU) or distributed if it takes at the different transmitters. Coordinated centralized beamforming approaches, where transmitters exchange both data and channel state information (CSI) for joint signal processing at the CU, promise larger spectral efficiency gains than distributed interference coordination techniques, but typically at the price of larger backhaul requirements and more severe synchronization requirements.

In this thesis we consider a distributed precoded multicell approach, where the precoders are computed locally at each BS to mitigate the intercell interference, assuming only the knowledge of the local CSI (i.e. the channels between a given BS and the cooperative users terminals). Two precoder are considered: distributed zero forcing (DZF) and distributed virtual signal-to-interference noise ratio (DVSINR) recently proposed. Then the system is further optimized by computing a power allocation algorithm over the subcarriers that minimizes the average bit error rate (BER), under per-BS power constraint. Both, upper and lower bounds, used to reduce the search space for the optimum solution and therefore efficiently perform the power allocation procedure, are derived.

The knowledge of CSI at the transmitter is absolutely crucial for the precoded-based systems. However, assuming perfect CSI at the transmitters is not realistic in many practical scenarios and thus in this thesis we also assess the performance of the precoders under imperfect CSI. A quantized version of the CSI associated to the different links between the BS and the UT is feedback from the UT to the BS. This information is then employed by the different BSs to perform the precoding design. A new DVSINR precoder explicitly designed under imperfect CSI is proposed. The considered schemes are implemented and evaluated under the LTE parameters and scenarios.

1.3. Structure

After presenting the evolution of wireless communications in the past years and its current status, where LTE is the main 4G standard already deployed in many countries, we present, in Chapter 2 “Multiple Carrier Schemes” and Chapter 3 “Multiple Antenna Techniques” the main enabling technologies of LTE.

Subsequently we present in Chapter 4 “Long Term Evolution System” the major aspects of the LTE system, namely its networks architecture and physical layer. Afterwards, in Chapter 5 “LTE-Advanced” we discuss the evolution of LTE systems, LTE-Advanced and its own enabling technologies. One of the enabling technologies of LTE-Advanced, and the main subject of this study is the concept known as Coordinated Multipoint, also known as CoMP. The main aspects of this concept are presented in a subchapter designated “Coordinated Multi-Point Transmission – CoMP”.

In Chapter 6 “Cooperative Schemes Implemented” we present the cooperative techniques developed in this thesis and evaluate their performance. The system model and the parameters used are defined. The main objective of this chapter is the use of distributed precoder vectors, and further optimization of the same. Also, a simple channel quantization technique is presented and used to evaluate the precoder techniques under imperfect CSI.

Finally, in Chapter 7 we conclude the work made throughout this thesis and provide some guidelines for future.

2. Multiple Carrier Schemes

Single Carrier (SC) transmission schemes modulate the information in only a carrier, adjusting the carriers phase or amplitude (or sometimes both). The higher the data rate, the higher the symbol rate in a digital system and thus the required bandwidth is higher [8].

Using medium access techniques based on frequency multiplexing – Frequency Division Multiple Access (FDMA), different users use different carrier frequencies to access simultaneously the communication system [8]. The biggest emphasis in the development of this type of system is on the mitigation of excessive interference between carriers, seeing that the transmitted signals are not sinusoidal. This suggests that if the channel is under-spread (the coherence time is bigger than the delay spread), it is then approximately invariant in time for a big enough time scale [9]. The use of such type of systems requires the usage of guard bands, which may render the system inefficient.

The solution for this interference, caused by the guard band requirements, passes by the selection of the system parameters that allow us to attain orthogonality between the different transistors, thus creating sub-carriers that don't interfere with each other, but whose spectrums may overlap in the frequency domain.

2.1. Orthogonal Frequency Division Multiplexing

The basic concept of OFDM (*Orthogonal Frequency Division Multiplexing*) is to divide the available spectrum in parallel narrowband channels, denominated by subcarriers, and sending information in this parallel channels, at a low transmission rate [3]. By doing so, each channel experiences flat-fading which leads to only some of the OFDM subcarriers being affected by the fades and thus, instead of losing the entire symbol, we just lose portions of the symbol and its recovery may be possible by using proper coding and error correction, simplifying a lot the frequency equalization. Although the frequency response of the several channels overlaps, they are orthogonal to each other, since the frequencies of the different subcarriers are chosen so that, in the frequency domain, the neighbor subcarriers have zero values for the sampling times of the required subcarrier.

In an OFDM system with N_C sub-carriers there will be transmitted N_C data symbols in parallel, each modulated in a different sub-carrier. Hence, the duration of an OFDM symbol is given by:

$$T_{OFDM} = N_C T_S \tag{2.1.1}$$

The frequency of a sub-carrier is given by:

$$f_k = k\Delta f \tag{2.1.2}$$

where Δf stands for the sub-carrier spacing, given by:

$$\Delta f = \frac{1}{T_{OFDM}} \tag{2.1.3}$$

Each carrier is modulated by a data symbol. An OFDM symbol is formed simply by the addition of the different modulated signals from the sub-carriers.

The OFDM system relays on digital technology, using the Fast Fourier Transform (FFT) and Inverse Fourier Transform (IFFT) to move the signal between the time and frequency domain, without the loss of information, assuming that the classical requirements for digital signal processing in terms of minimum sampling rates and word lengths are fulfilled [8].

2.1.1. Orthogonality

As stated previously, in order for a receiver to separate the overlapped subcarriers without interference, said subcarriers must be orthogonal to each other. The property of orthogonality allows simultaneous transmission of additional subcarriers in a tight frequency space without interference from each other, thus being the main advantage of OFDM.

The definition of orthogonality is stated in the following equation:

$$\int_0^T S_i(t).S_j(t)dt = \begin{cases} C \ if \ i = j \\ 0 \ \ if \ i \neq j \end{cases} \tag{2.1.4}$$

In other words, what this equation represents is that if we have two different functions and multiply and integrate them, over a symbol period, the result is null if the functions are orthogonal to each other.

The most basic form of modulation applied to the subcarriers is square wave phase modulation, which produces a frequency spectrum represent by a $sinc(fT)$ function [4], that is characterized by having a maximum amplitude at the center and null amplitude in multiples of $1/T$, where T is the duration of the modulated symbol. What makes OFDM a practical transmission system is that we can match the subcarrier modulation rate to the subcarrier spacing such that the nulls in the spectrum of one subcarrier line up with the peaks of the adjacent subcarriers.

2.1.2. Cyclic Prefix

The orthogonality of the OFDM sub-carriers can be lost when the signal passes through a time dispersive channel, due to inter-symbolic interference, seeing that the symbol do not confine to their time slots, spreading over the next slots. Nevertheless, a cyclic extension of the OFDM signal can be made so to avoid interference [10].

The cyclic prefix is a guard time, bigger than the maximum time delay of the different radio channel paths. The last part of the sequence is replicated in the guard time, on the beginning of the OFDM symbol. The addition of this prefix makes the transmitted OFDM symbol periodic, and helps avoid inter-symbolic interference, since all the samples in the slot (0 to T_{OFDM}) undergo the same type of interference. The periodic nature of the signal also allows for a discrete Fourier spectrum, enabling the use of DFT and IDFT in the receiver and transmitter respectively. [8]

Within each OFDM symbol the guard period added increases the length of the symbol waveform, being the total length given by:

$$T_{symbol} = T_g + T_b \tag{2.1.5}$$

where T_g is the length of the guard period and T_b the useful symbol time corresponding to the size of the IFFT that generated the OFDM signal. The figure bellow shows the structure of the OFDM symbol.

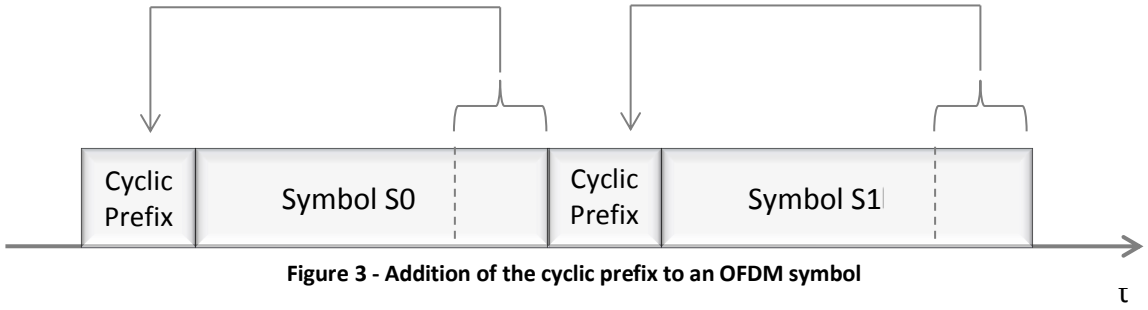

Figure 3 - Addition of the cyclic prefix to an OFDM symbol

The length of the Cyclic Prefix is chosen regarding a compromise between the increase of energy transmitted due to the increase of the CP length, thus causing a loss in the SNR, and having its length corresponding at least to the offset between the slowest and fastest subcarrier to make the received subcarrier unaffected by any dispersion to avoid both ISI and ICI.

Despite this method benefits in terms of limitation of inter-symbolic interference, the utilization of a cyclic prefix implies a certain loss of spectral efficiency, since it reduces the transmission rate.

The loss of SNR caused by the insertion of the CP, depicted previously, is described in equation (2.1.6).

$$SNR_{loss\,[dB]} = -10log_{10}\left(1 - \frac{T_g}{T_{symbol}}\right) \tag{2.1.6}$$

The duration of the short and long cyclic prefix for the LTE is 4.7μs and 16.7μs respectively [10]. The OFDM symbol period is of $T_b = 66.67\mu s$, so according to equations (2.1.5) and (2.1.6), we

get that SNR_{loss} for the short CP is of 1.0708 and 1.25 for the long CP. In terms of spectral efficiency, given by $\eta = SNR_{loss}^{-1}$, the short CP has a spectral efficiency of 93.4% and the long 80%.

2.1.3. Modulation

The basic principle of multicarrier modulation is to divide the available bandwidth, B, into a number N_C sub-bands, or subcarriers. Each one of this subcarriers has a width of $\Delta f = W/N_C$. So, instead of transmitting the data stream in a serial way, at a baud rate of R, a multicarrier modulation scheme splits the data symbols into blocks of N_C data symbols, which are then transmitted in parallel, by modulating the N_C subcarriers. The duration of a multicarrier scheme symbol is then given by $T_{symbol} = N_C/R$.

When we add more subcarriers the symbol period increases and, therefore, the data stream becomes more robust to channel distortion, impulse noise and fading. Those channel effects could result in inter-symbolic interference (ISI) when the time dispersion becomes significant, compared to the symbol period.

2.1.4. OFDM System

An OFDM system uses the properties of the OFDM concept presented previously in order to enable that multiple users can access the shared medium.

The concept of such approach is that the symbols to be transmitted from one BS towards multiple UT are modulated in the frequency domain, mapped to different sub-carriers and then an IDFT is used to generate a time domain signal. A cyclic prefix, as described previously, is inserted before each orthogonal frequency division multiplex (OFDM) symbol, in order to assure that even a channel with large delay spread does not cause ISI, and that a transmission leads to a circularly symmetric convolution of the transmitted samples with the channel. Each receiving UE can then discard the cyclic prefix, perform a DFT, and obtain (scaled and noisy) transmitted symbols in the frequency domain again.

In LTE the subcarrier spacing is $\Delta f = 15\,\mathrm{kHz}$ with a cyclic prefix (CP) duration of $T_{CP} \approx 4.7/16.7\mu s$ (short/long CP) [10], regardless of the total available bandwidth. Since the subcarriers are orthogonal to each other when the sampling is done, the other subcarriers will have zero value.

The transmitter of an OFDMA system uses IFFT blocks to create the signal. Each input for the IFFT block corresponds to the input representing a particular subcarrier and can be modulated independently of the other subcarriers. This is followed by a Cyclic Extension, whose purpose was explained previously. The cyclic prefix makes the OFDM symbol periodic, allowing a Fourier spectrum, which enables the use of IFFT at the transmitter and FFT at the receiver.

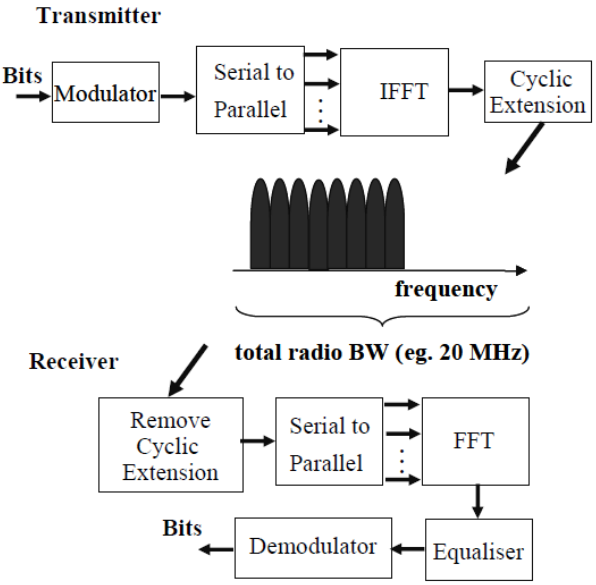

Figure 4 - Transmitter and Receiver of an OFDMA system [8]

At the receiver the cyclic prefix must be removed. Although this guard interval protects the symbol against ISI, each subcarrier may be affected by different amplitude and phase changes, due to the channel impact. In order to account this kind of effects, pilot symbols are added, with proper placement in both time and frequency domain, to the OFDM symbol. These pilot symbols are known references that form a time and frequency domain grid, which facilitate the channel estimation, so that the receiver can interpolate the effects of the channel to the different subcarriers. An example of said grid is presented in the figure bellow.

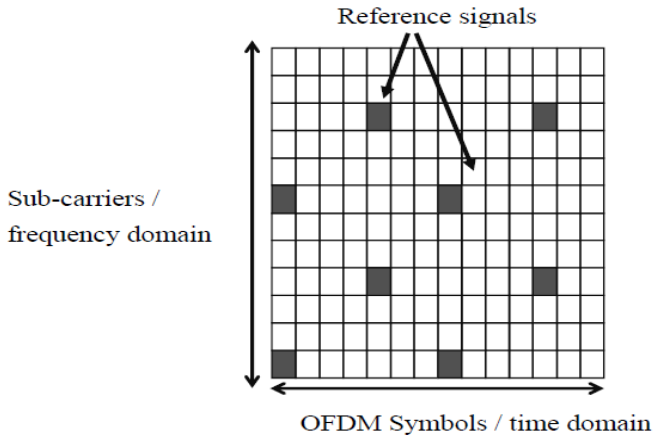

Figure 5 - Reference symbols spread over OFDMA subcarriers and symbols

A typical type of receiver solution is the frequency domain equalization, which basically reverts the channel impact for each subcarrier. In OFDMA this means to simply multiplying each subcarrier (with the complex valued multiplication) based on the estimated channel frequency response (the phase and amplitude adjustment each subcarrier has experienced) of the channel [8].

One last assignment that the OFDM receiver must accomplish is time and frequency synchronization, which allows the correct frame and OFDM symbol timing to be obtained so that the correct part of the received signal is dropped. While time synchronization is achieved by the correlation between the known data samples (typically the pilot symbols) and the actual received data, for frequency synchronization the frequency offset between the transmitter and the receiver is estimated by using an estimation of the frequency offset between the UT and the BS, where the UT locks to the frequency obtained from the BS.

A time and frequency representation of an OFDM symbol is presented below.

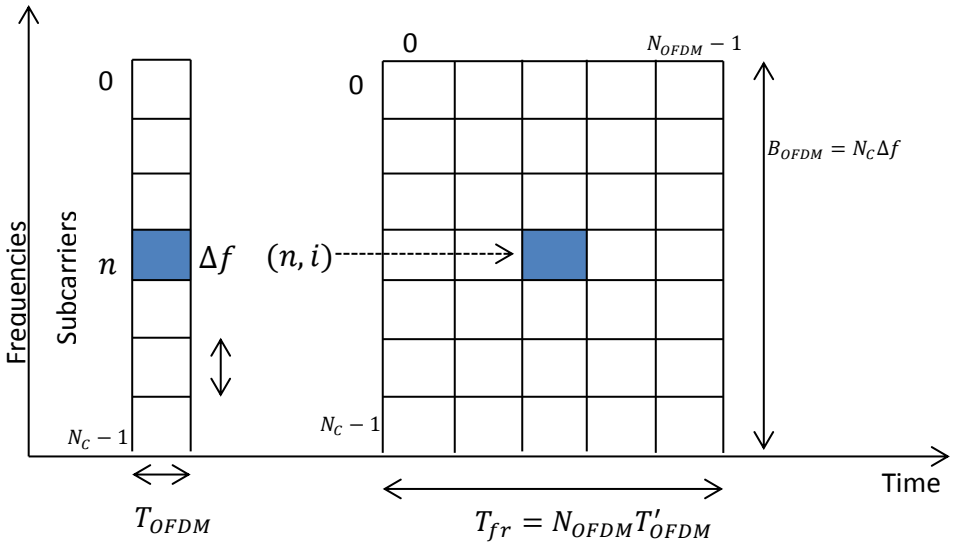

Figure 6 - OFDM symbol

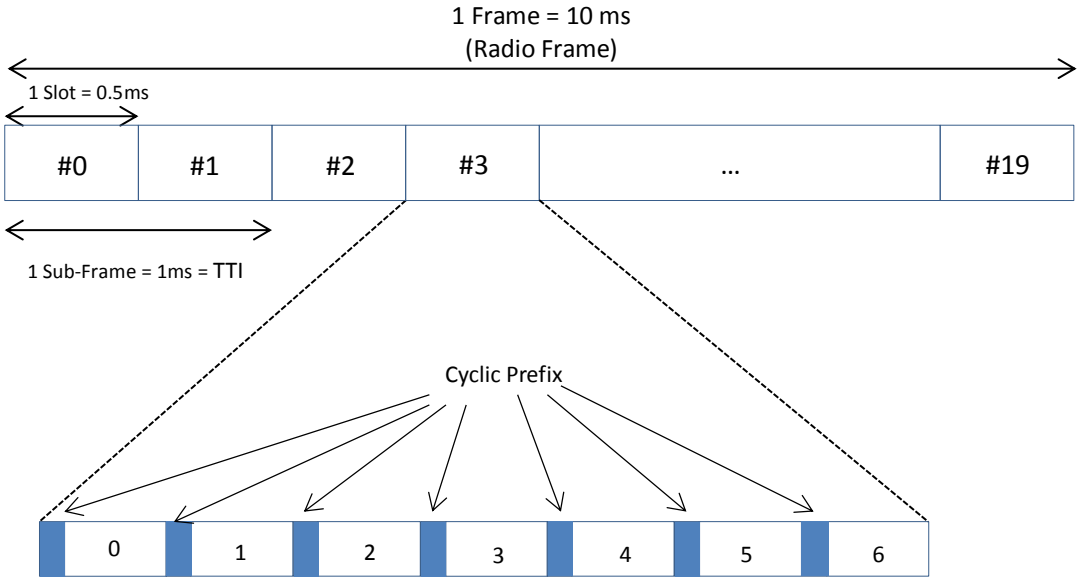

Figure 7 - LTE generic frame structure

2.2. OFDMA

Orthogonal Frequency-Division Multiple Access (OFDMA) is a multi-user version of the digital modulation scheme stated previously, OFDM. It distributes different sets of subcarriers, allocated in continuous groups or distributed, to different users at the same time.

The usage of an OFDMA system in mobile communications came from the fact that the transmissions, occurring in a shared medium, susceptible to rich scattering, needed a simple and flexible access for a high number of communication entities. There was a need for a low-cost and efficient signal processing solution that can divide a mobile communications system into a large number of flexible bit pipes, according to the many users' needs. The standard for mobile communications, LTE, uses an OFDMA approach to deal with the matters stated previously.

One of the OFDMA features is the capacity of mapping subcarriers in two different matters, in continuous groups or in a distributed manner. We can see in the figure bellow the difference between this two types of subcarrier mapping. By using the later we are able to exploit multiuser diversity.

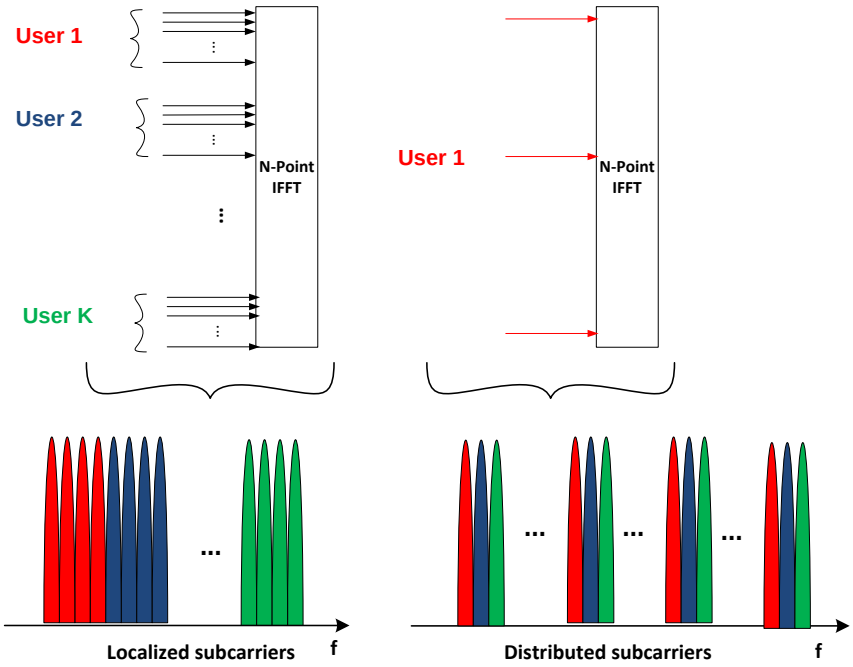

Figure 8 - Subcarriers' mapping

2.2.1. Advantages

While being computationally inexpensive and sacrificing only a reasonable extent of capacity for the cyclic prefix, OFDMA has the advantage of being easily designed to fulfill different spectral masks through an appropriate choice of guard bands, it is able to avoid ISI and inter-carrier-wise equalization at the receiver side and is highly suitable for multiple access.

2.2.2. Disadvantages

The OFDMA system may present some disadvantages, being the most relevant one that of a high peak-to-average power ratio (PAPR), due to the performance of modulation on the frequency domain and the application of an IDFT. In the uplink, this aspect may be critical as it implies that a large power amplifier (PA) back-off is needed, leading to a faster depletion of handset battery. To cope with this problem, 3GPP decided to employ single carrier frequency domain multiple access (SC-FDMA) in the uplink, where modulation is performed in the time domain, after which a small DFT is applied and the signals are mapped to the sub-carriers to be used by the terminal before the actual large IDFT.

3. Multiple Antenna Techniques

Multiple antenna techniques allow base stations and mobile equipment's to use multiple antennas in radio transmissions and receptions, in order to increase data rates and performance, or reduce ISI and interference from other users. There are three main multiple antenna techniques, which have different objectives and are implemented in different ways.

One of the most used techniques is diversity processing, which increases the received signal power and reduces the amount of fading by using multiple antennas at the transmitter, the receiver, or both. In spatial multiplexing, also known as MIMO (Multiple Input Multiple Output), the transmitter and receiver both use multiple antennas in order to increase the systems data rates. Lastly, beamforming uses multiple antennas at the base station in order to separate the users that share the same resources; this can be seen as a multiple access technique referred as space division multiple access (SDMA).

There are three multi-antenna configurations, which allow exploiting both diversity and spatial multiplexing, depending on the number of antennas in both the transmitter and the receiver, MISO (Multiple Input Multiple Output), SIMO (Single Input Multiple Output) and MIMO (Multiple Input Multiple Output). The figure bellow illustrates these different schemes. The SISO system is also added to comparison.

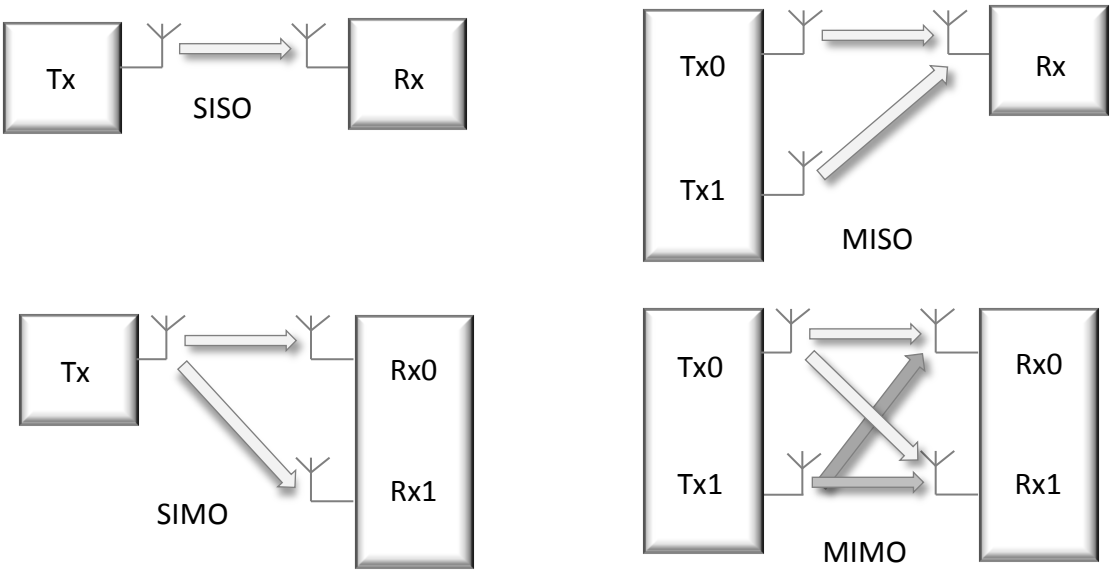

Figure 9 - Multiple Antennas Schemes

Single-input single-output (SISO) is the well-known, typical wireless configuration, single-input multiple-output (SIMO) is the configuration where a single transmitting antenna and multiple receiving antennas (M_R) are used, multiple-input single-output (MISO) has multiple (M_T) transmitting antennas and one receiving antenna and MIMO has multiple (M_T) transmitting and receiving (M_R) antennas.

Multiple antenna configurations can also be used to separate the users that share the same resources, being usually called as multiuser MIMO (MU-MIMO), which refers to a configuration that comprises a base station with multiple transmit/receive antennas interacting with multiple users, each equipped with single or multiple antennas. This scheme is depicted in the figure bellow.

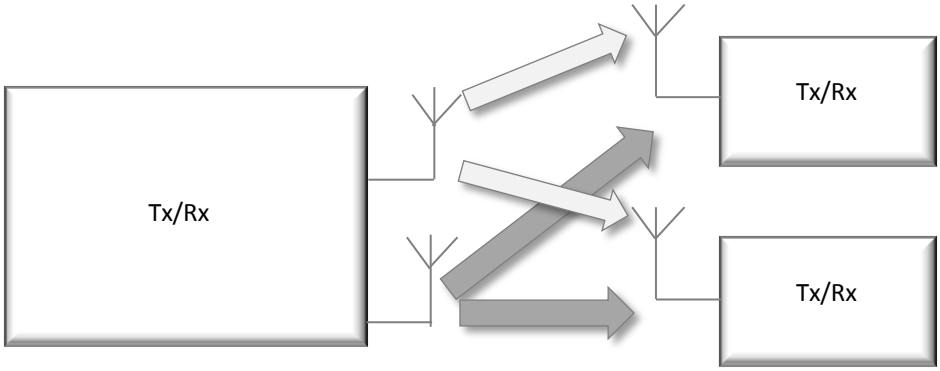

Figure 10 - MU-MIMO Scheme

3.1. Spatial Multiplexing

Spatial multiplexing is often described as the use of MIMO antennas. This name is derived from the inputs and outputs to the air interface, so that multiple inputs refer to the transmitter and multiple outputs to the receiver. So, if the transmitter and the receiver both have multiple antennas, then we can set up multiple parallel data streams between them, in order to increase the data rate.

Spatial multiplexing offers a linear increase in the transmission rate (or capacity) for the same bandwidth and with no additional power expenses, by splitting the bit stream into two half-rate bit streams, modulated and transmitted simultaneously from both antennas. The receiver, having knowledge of the channel, recovers these individual bit streams and combines them so as to recover the original bit stream. In a system with M_T transmit antennas and M_R receive antennas, often known as a $M_T \times M_R$ spatial multiplexing system, the peak data rate is proportional to $\min(M_T, M_R)$ [11].

This concept can be extended to MU-MIMO. In such a case, two users can transmit simultaneously their respective information to the base station equipped with two antennas. The base station can then separate the two signals and, likewise, transmit two signals with spatial filtering so that each user can decode its own signal correctly. By doing so, we can increase the system's capacity proportionally to the number of antennas at the base station and the number of users.

Let us consider the system model represented in the following figure, assuming that the CSI is available at the transmitter:

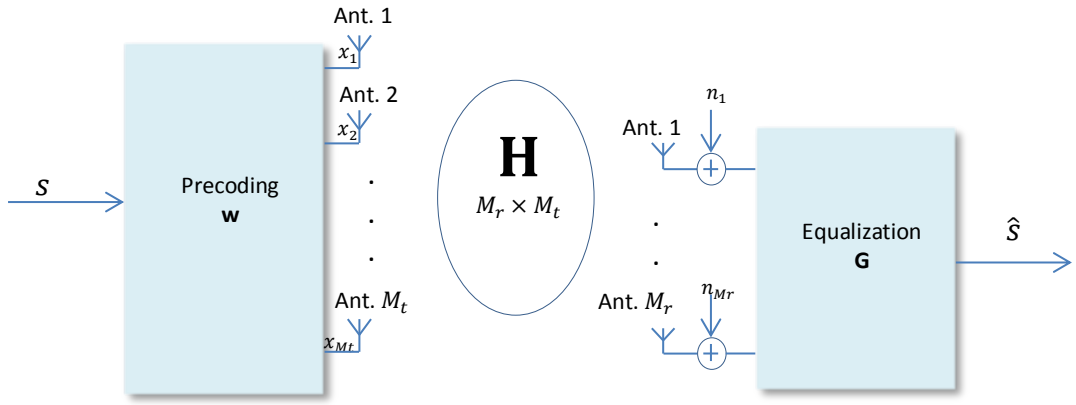

Figure 11 - Spatial Multiplexing

In matrix notation, what we can see in the figure is represented by:

$$\boldsymbol{y} = \mathbf{H}\mathbf{x} + \mathbf{n} \tag{3.1.1}$$

where $\boldsymbol{x} = [x_1 \dots x_{Mt}]^T$ is the sent signals vector, with size $M_t \times 1$, $\boldsymbol{y} = [y_1 \dots y_{Mr}]^T$ is the received signal vector, with size $M_r \times 1$,

$$\mathbf{H} = \begin{bmatrix} h_{11} & \dots & h_{1Mt} \\ \vdots & h_{ij} & \vdots \\ h_{Mr1} & \dots & h_{MrMt} \end{bmatrix}, i = 1, \dots, M_r, j = 1, \dots, M_t \tag{3.1.2}$$

is the MIMO channel matrix, with size $M_t \times M_r$; $\boldsymbol{n} \sim \mathcal{CN}(0, \sigma^2 I_{M_r})$ represents the noise vector.

The MIMO channel can be converted into a set of parallel channels. This can be done by decomposing the $\mathbf{H}$ matrix, using the singular value decomposition (SVD), as

$$\mathbf{H} = \mathbf{U}\mathbf{D}\mathbf{V}^H \tag{3.1.3}$$

where $\mathbf{U}$ and $\mathbf{V}$ are unitary matrices of size $M_r \times r$ and $M_t \times r$ ($r = rank(\mathbf{H}) \leq \min(M_t, M_r)$) and $\mathbf{D}$ is a diagonal matrix whose elements are non-negative real numbers,

$$\mathbf{D} = \begin{bmatrix} \lambda_1 & 0 & 0 \\ 0 & \ddots & 0 \\ 0 & 0 & \lambda_r \end{bmatrix} \tag{3.1.4}$$

Setting the precoding matrix, $\mathbf{W}$ as,

$$\mathbf{W} = \mathbf{V}\mathbf{P}^{1/2} \tag{3.1.5}$$

with size $M_t \times r$, where $\mathbf{P}$ is a square diagonal power allocation matrix of size $r \times r$

$$\mathbf{P} = \begin{bmatrix} \mathrm{p}_1 & 0 & 0 \\ 0 & \ddots & 0 \\ 0 & 0 & \mathrm{p}_\mathrm{r} \end{bmatrix}^{1/2} \tag{3.1.6}$$

The equalizer matrix $\mathbf{G}$ is set as,

$$\mathbf{G} = \mathbf{U}^H \tag{3.1.7}$$

So, the transmitted signal over the M_t antennas is given by,

$$\mathbf{x} = \mathbf{W}\mathbf{s} \tag{3.1.8}$$

where $\boldsymbol{s} = [s_1 \quad \cdots \quad s_r]^T$ is the data vector of size $r \times 1$. Replacing $\mathbf{W}$ and $\mathbf{H} = \mathbf{U}\mathbf{D}\mathbf{V}^H$ on the received signal we get

$$\boldsymbol{y} = \mathbf{U}\mathbf{D}\mathbf{V}^H\mathbf{V}\mathbf{P}^{1/2}\boldsymbol{s} + \boldsymbol{n} \tag{3.1.9}$$

The estimated transmitted data symbols can then be obtained as,

$$\hat{\boldsymbol{s}} = \mathbf{G}\mathbf{y} = \mathbf{U}^H\mathbf{U}\mathbf{D}\mathbf{V}^H\mathbf{V}\mathbf{P}^{1/2}\boldsymbol{s} + \mathbf{U}^H\boldsymbol{n} \tag{3.1.10}$$

$$\hat{\boldsymbol{s}} = \mathbf{D}\mathbf{P}^{1/2}\boldsymbol{s} + \tilde{\boldsymbol{n}} \tag{3.1.11}$$

The soft estimate of the rth data symbol is,

$$\hat{\mathbf{s}}_\mathbf{i} = \boldsymbol{\lambda}_\mathbf{i}\sqrt{\mathbf{p}_\mathbf{i}}\mathbf{s}_\mathbf{i} + \tilde{\mathbf{n}}_\mathbf{i}, \ \mathbf{i} = \mathbf{1}, \dots, \mathbf{r} \tag{3.1.12}$$

As we can see, the estimated data symbol is free of interference, being only affected by noise. So, converting MIMO channels into r parallel channels through SVD allows us to transmit r parallel, interference free, data symbols.

3.2. Diversity

Diversity means that the same information can be sent over different independent paths, and can be obtained in time, frequency and space. The main idea behind the diversity concept is to send the same information bits through different fading paths and then combine the information received over these paths in the receiver, in order to mitigate the fading effects.

Time diversity consists of sending the same information in different time periods, separated by time intervals bigger than the coherence time. In general, with very short transmission time of 1ms subframe in the LTE system, there is not much time-diversity available (except for the case of

very high UT speeds) [3]. The biggest setback of time diversity is the fact that it diminishes the data rates, due to its data repetition.

On the other hand, frequency diversity enables the transmission of the same narrow-band signal in different carriers, separated by a coherence bandwidth. In LTE systems, it can be exploited by scheduling transmissions over distributed resources. However this type of diversity requires the use of more bandwidth.

3.2.1. Receive Diversity

Receive diversity is most often used in the uplink, where the base stations use multiple antennas to pick up more copies of the received signal. The signals that reach the receiver antennas have different phase shifts, but they can be removed by antenna-specific channel estimation. The base station can then add the signals together in phase, without risking destructive interference between them.

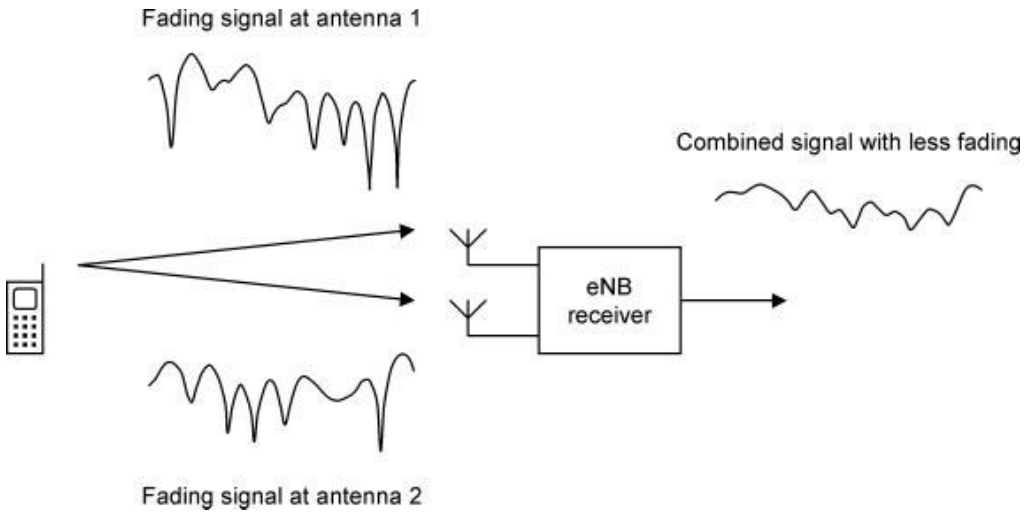

Figure 12 - Reducing fading by using receiver diversity [3]

Both signals, due to the existence of obstacles between the transmitting and the receiving antennas, are subject of fading. The effects of that fading will generate different paths for the transmitted data, which are received with temporal variations of amplitude and phase. If the two individual signals undergo fades at the same time, then the power of the combined signal will be low. But if the antennas are far enough apart (a few wavelengths of the carrier frequency), [2] then the two sets of fading geometries will be very different, so the signals will be far more likely to undergo fades at completely different times. Thus, we have reduced the amount of fading in the combined signal, which in turns reduces the error rate.

It is usual for base stations to have more than one receive antenna. In LTE, the mobile's test specifications assume that the mobile uses two receive antennas [12], so the systems are expected to use receive diversity on both downlink and uplink. A mobile's antennas are closer together than

those of a base station, so the benefits of receive diversity are reduced, but the situation can often be improved using antennas that measure two independent polarizations of the incoming signal.

A list, of the most common receive diversity schemes, is presented below:

- **Selection Combining –** The receiver selects the antenna with the highest received signal and ignores the signal received from the other antennas.
- **Switched Combining –** The receiver sets a SNR threshold and if the received signal at a determined antenna is above that value, than it is selected until it drops again under that threshold.

It is also very common to use frequency equalizers, and the most used are presented below:

- **Equal Gain Combining –** the received signals from the multiple receiving antennas are summed up coherently, compensating the phase rotation caused by the channel.
- **Maximum Ratio Combining –** the received signals from the different antennas are weighted individually depending on the reliability of the signal in each antenna and then the phase distortion is compensated by calculating the complex conjugate of the frequency response of the channel. Afterwards the signals are aligned and combined.
- **Zero Forcing Combining –** designed for each data symbol in order to remove the interference, by restoring the orthogonality between users inverting the channel frequency response. However, this equalizer boosts the noise when the frequency response of the channel is in deep fading.
- **Minimum Mean Square Error Combining –** it minimizes the mean square error between the transmitted and estimated signal. It is a trade-off between noise enhancement and interference removal. For high SNR, this equalizer tends to the ZF.

3.2.2. Transmit Diversity

Transmit diversity reduces the amount of fading by using two or more antennas at the transmitter. It is a process very similar to the Receive Diversity, but with a crucial problem: the signals add together at the single receive antenna, which brings a risk of destructive interference. This problem can be copped with in two ways, closed loop transmit diversity, where CSI is available at the transmitter side, or open loop transmit diversity, where contrarily to the previous case, CSI is not available at the transmitter.

In closed loop transmit diversity, the transmitter sends two copies of the signal in the expected way, but it also applies a phase shift to one or both signals before transmitting them, thus ensuring that the two signals reach the receiver in phase, without any risk of destructive interference. The phase shift is determined by a precoding matrix indicator (PMI), which is calculated by the receiver and fed back to the transmitter. The PMI might indicate two options: either transmit

both signals without any phase shift, or transmit the second with a phase shift of 180º. If this first option leads to destructive interference the second option will automatically work.

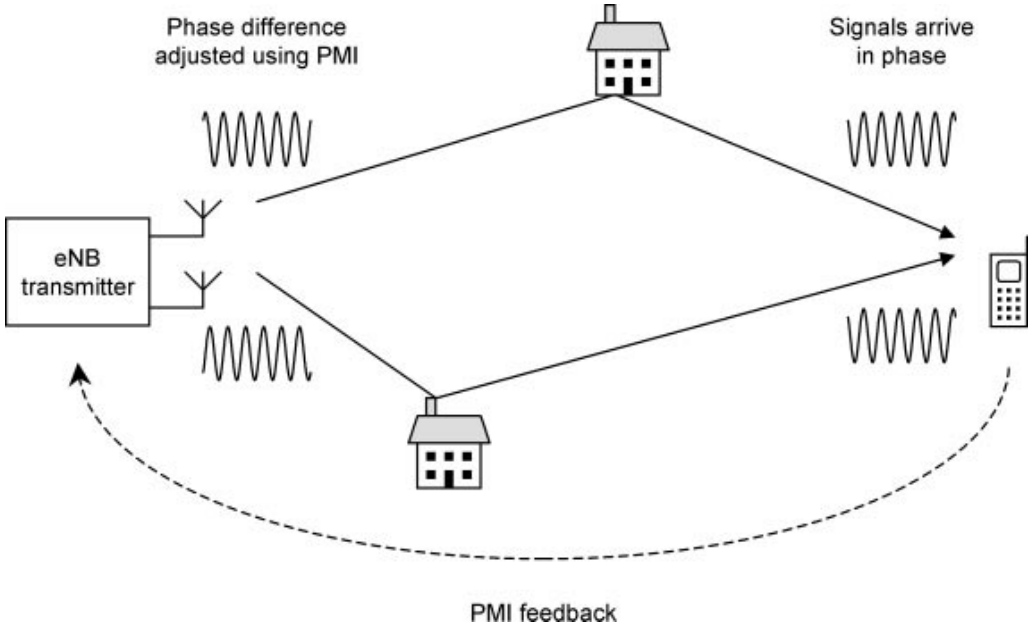

Figure 13 - Open loop Transmit Diversity

The phase shifts introduced by the radio channels depend on the wavelength of the carrier signal, and so, on its frequency. The PMI choice depends on the position of the mobile, so a fast moving mobile will have a PMI that frequently changes. Regrettably, the feedback loop introduces time delays into the system, so in the case of fast moving mobiles, the PMI may be out of date by the time it is used. That being so, closed loop transmit diversity is only suitable for mobiles that are moving sufficiently slowly. So, for fast moving mobiles it is better to use open loop techniques.

Open loop techniques are based primarily on the use of Space-time/frequency block coding (STBC/SFBC), that offer significant gains in signal robustness under fading channel conditions, but it doesn't improve data rates. STBC/STFC makes use of either Alamouti schemes or Tarokh Codes. Alamouti schemes use simpler coding schemes based on orthogonal codes for two transmit antennas and M receiver antennas ($2 \times M$), with no bandwidth expansion. Tarokh Codes are orthogonal codes for more than two transmit antennas but require bandwidth expansion.

The use of STBC involves the duplication of data onto multiple antennas [4]. The signals used for additional antennas are distinguished by a combination of reversing the time allocation and applying a complex conjugation to part of the signal. SFBC uses the Alamouti's technique [13] but copies data onto different frequencies instead of using blocks of time. In LTE only SFBC is used.

3.2.2.1. Alamouti Scheme

In the Alamouti approach, the information bits are first modulated using an M-ary modulation scheme. The encoder then takes a block of modulated symbols s_n and s_{n+1} in each encoding operation and gives it to the transmitter antennas according to the code matrix,

$$\mathbf{S} = \begin{bmatrix} s_n & -s_{n+1}^* \\ s_{n+1} & s_n^* \end{bmatrix} \quad (3.2.1)$$

The matrix first column represents the first transmission period and the second column the respective second transmission period. On the other hand, the first row corresponds to the symbols transmitted by the first antenna, while the symbols in the second row correspond to the symbols transmitted by the second antenna. (The symbol * denotes that the transmitter should change the sign of the quadrature component, in a process known as complex conjugation).

More specifically what happens is that, during the first symbol period, the first antenna transmits s_n and the second one transmits s_{n+1}.During the second symbol period, the first antenna transmits $-s_{n+1}^*$ and the second antenna transmits s_n^*.

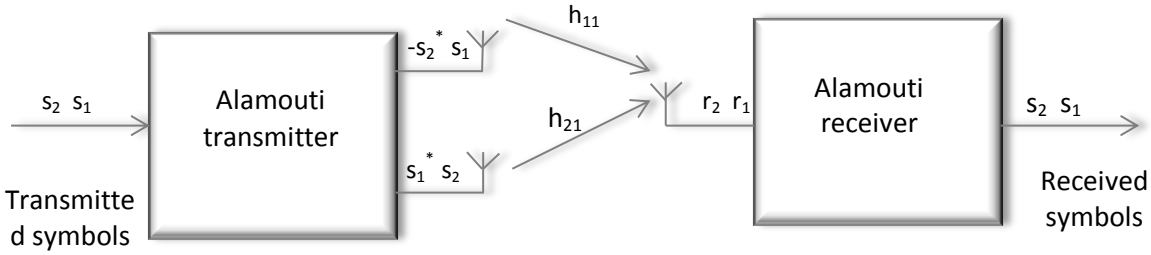

Figure 14 - Block diagram of the Alamouti Scheme with two transmitter antennas and one receiving antenna

This implies that we are transmitting both in space (across two antennas) and time (two transmission intervals). By doing so, the receiver can now make two successive measurements of the received signal, which corresponds to two different combinations of the symbols s_n and s_{n+1}.[14]

Looking at the following equations, where $\mathbf{s_n}$ is the information sequence from the first antenna and $\mathbf{s_{n+1}}$ is the information sequence from the second antenna,

$$\mathbf{s_n} = [s_n, \quad -s_{n+1}^*] \quad (3.2.2.)$$

$$\mathbf{s_{n+1}} = [s_{n+1}, \quad s_n^*] \quad (3.2.3)$$

Examining the previous equations, it's easy to see that the sequences are orthogonal (i.e., the inner product of $\mathbf{s_n}$ and $\mathbf{s_{n+1}}$ is zero). This inner product is given by,

$$s_n s_{n+1} = s_n s_{n+1}^* - s_{n+1}^* s_n = 0 \quad (3.2.4)$$

Considering H_1 the channel response between the first transmitting antenna and the receiver and H_2 the channel response between the second transmitting antenna and the receiver, they both form the vector $\mathbf{h} = [h_1 \quad h_2]^T$.

Being so, the received signal is given by,

$$\mathbf{Y} = \frac{1}{\sqrt{2}}\mathbf{S}\mathbf{h} + \mathbf{n} \tag{3.2.5}$$

considering that is the channel noise vector, composed by $\mathbf{n} = [n_n \quad n_{n+1}]$, where n_n and n_{n+1} are independent complex variables with zero mean and unit variance, representing additive white Guassian noise samples, at time t and $t + T$, respectively. Each symbol is multiplied by a factor of a squared root of two in order to achieve a transmitted average power of one in each time step.

The previous equation can be decomposed in:

$$\begin{cases} y_n = \frac{1}{\sqrt{2}}h_{1,n}s_n - \frac{1}{\sqrt{2}}h_{2,n}s_{n+1}^* + n_n \\ y_{n+1} = \frac{1}{\sqrt{2}}h_{1,n}s_{n+1} + \frac{1}{\sqrt{2}}h_{2,n+1}s_n^* + n_{n+1} \end{cases} \tag{3.2.6}$$

Since OFDM systems were designed in order to flatten the fading in each subcarrier, we can assume that $h_{k,n} = h_{k,n+1}$. Thus, and considering the previous equality, the decode estimated symbols are given by,

$$\begin{cases} \hat{s}_n = \frac{1}{\sqrt{2}}h_1^* y_n + \frac{1}{\sqrt{2}}h_2 y_{n+1}^* \\ \hat{s}_{n+1} = -\frac{1}{\sqrt{2}}h_2 y_n^* + \frac{1}{\sqrt{2}}h_1^* y_{n+1} \end{cases} \tag{3.2.7}$$

The soft decision of data symbol s_n is then given by,

$$\hat{s}_n = \frac{1}{2}(h_1^* h_1 + h_2 h_2^*)s_n + \frac{1}{\sqrt{2}}h_1^* n_n + \frac{1}{\sqrt{2}}h_2 n_{n+1}^* \tag{3.2.8}$$

Thus, we can see that the interference caused by the $n + 1$ data symbol is fully eliminated. The SNR can is given by:

$$SNR = \frac{1}{2}\frac{(|h_1|^2 + |h_2|^2)}{\sigma^2} \tag{3.2.9}$$

There is no equivalent to Alamouti's technique for systems with more than two antennas but, despite that, diversity can be achieved in four antenna systems, by swapping back and forth between the two constituent antenna pairs. This technique is used in LTE for four antenna open loop diversity.

3.3. Beamforming

Beamforming is a general signal processing technique used to control the directionality of the reception or transmission of a signal. In cellular communication systems, base station's antennas work together, as an array, in order to create a synthetic directional antenna beam, which has a main

beam pointing at a given UT, and a null pointing towards the other UTs. The beam width is narrower than one from a single antenna, so the transmitter power is focused towards the intended UT. As a result, we can increase the range of a base station in the direction of said UT. This is achieved by combining elements in a phased array in such way that at particular angles the antennas signals experience constructive interference while others experience destructive interference.

So, it is possible to adjust the amplitudes and phases of the transmitted signals, by applying a suitable set of antenna weights. In a system with N antennas, this allows us to adjust the direction of the main beam and up to $N - 2$ nulls or side lobes [2].

Figure 15 - Beamforming [14]

In OFDMA, we are able to process different sub-carriers using different sets of antenna weights, in order to create a synthetic antenna beam directed at any direction. It is then possible to communicate with several different mobiles at once, using different subcarriers, even if those mobiles are in completely different locations.

The use of beamforming works best if the antennas are close together, with a separation comparable with the wavelength of the radio waves, because it ensures that the signals sent or received by the antennas are highly correlated. This is a different situation from diversity processing or spatial multiplexing, which work best if the antennas are far apart, with uncorrelated signals. A base station is therefore likely to use two sets of antennas: a closely spaced set for beamforming and a widely spaced set for diversity and spatial multiplexing.

4. Long-Term Evolution System

In this Chapter we briefly present the LTE standard, also known as 4G cellular systems. The goal of LTE is to provide a high-data-rate, low-latency and packet optimized radio-access technology supporting flexible bandwidth deployments [15].In order to support packet-switched traffic with seamless mobility, a new network architecture was designed, simplified into a IP based system, increasing the quality of service and reaching a minimum latency.

In the previous cellular systems, there were some fragmentations between different standards used. The second generation of cellular systems had TDMA based GSM and CDMA based IS-95, the third generation had UMTS and CDMA2000. But now, with the introduction of LTE, the fourth generation of cellular systems has a global standard. The first LTE proposal was in 2004 by NTT DoCoMo of Japan but the standard was only created in 2005. The world's first publicly available LTE service was lunched by TeliaSonera in Oslo and Stockholm on December 14, 2009 [16].

LTE was required to deliver a peak data rate of 100Mbps in the downlink and 50Mbps in the uplink. This requirement was exceeded in the eventual system, which delivers peak data rates of 300Mbps and 75Mbps respectively. For comparison, the peak data rate of WCDMA, in Release 6 of the 3GPP specifications, is 14Mbps in the downlink and 5.7Mbps in the uplink [2]. However, this peak data rates can only be achieved in optimal conditions, and are hard to achieve in a realistic scenario.

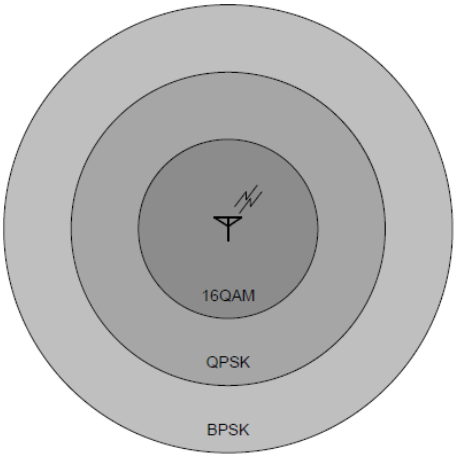

Figure 16 - Diagram of LTE UL selection of modulation scheme [15]

Within the specifications of the LTE system, there's a support for flexible bandwidth, thanks to the OFDMA and SC-FDMA access schemes. In addition to FDD (Frequency Division Duplexing) and

TDD (Time Division Duplexing), half-duplex FDD is also allowed to support low cost UTs. Unlike FDD, in a half-duplex FDD operation a UT is not required to transmit and receive at the same time, thus avoiding the need for a costly duplexer in the UT. The system is optimized for low speeds, up to 15km/h. However, the system specifications allow mobility support in excess of 350km/h with some performance degradation.

Since OFDMA has high PAPR, it requires inefficient power amplifiers and it would reduce the autonomy of mobile devices significantly. Being so, the uplink access is based on single carrier frequency division multiple access (SC-FDMA) that promises increased uplink coverage due to low PAPR relatively to OFDMA. While maintaining the same site location deployed in HSPA, the LTE system was able to improve the cell-edge throughput, and can have cell coverage between 5 and 100km. In terms of latency, the LTE radio-interface and network provides capabilities for less than 10ms latency for the transmission of a packet from the network to the UE.

Also defined in the standard, there are several modulation schemes available for the transmission of data. Higher modulation orders increase the data rate with the inconvenient of being more susceptible to signal errors and path loss. This means that the distance between the base stations and the mobile terminals matters in the selection of the modulation scheme. For the downlink the main modulation schemes supported are QPSK, 16-QAM and 64-QAM, while for the uplink 64-QAM is optional at the UT. Figure 16 illustrates the selection of modulation scheme, according to the SNR, assuming that a greater distance implies a lower SNR.

The principal system attributes of the LTE system are summarized in the next table:

Table 1 - LTEs' system attributes [3]

Bandwidth		1.25 – 20 MHz
Duplexing		FDD, TDD, half-duplex FDD
Mobility		350km/h
Multiple Access	Downlink	OFDMA
	Uplink	SC-FDMA
MIMO	Downlink	2 x 2, 4 x 2, 4 x 4
	Uplink	1 x 2, 1 x 4
Peak data rate in 20MHz	Downlink	173 and 326 Mb/s for 2 x 2 and 4 x 4 MIMO respectively
	Uplink	86Mb/s with 1 x 2 antenna configuration
Latency		< 10ms
Modulation		QPSK, 16-QAM and 64-QAM
Channel coding		Turbo code
Other techniques		Channel sensitive scheduling, link adaptation, power control, ICIC and hybrid ARQ

4.1. Network Architecture

LTE, being the evolution of the 3G systems, has, not only a new radio access interface (Evolved UMTS Terrestrial Radio Access Network – E-UTRAN), but also a simplified network architecture, designated System Architecture Evolution (SAE).

The LTE network architecture, SAE, is designed with the objective of supporting packet-switched traffic, with continuous mobility, quality of service (QoS) and minimal latency. This kind of approach allows the support for all required services, including voice trough packet connections. Subsequently, we have a highly simplified flat architecture, with only two types of nodes involved, namely the Node-B (eNB) and mobility management entity/gateway (MME/GW). This is in contrast with the many more network nodes in the previous 3G systems. One major change is that the radio network controller (RNC) is eliminated from the data path and its functions are now incorporated in the eNB. Having a single node in the access network reduces the latency and distributes the RNC processing load into multiple eNBs. The elimination of the RNC in the access network was possible partly because the LTE system does not support macro-diversity or soft-handover.

All the network interfaces are based on IP protocols. The eNBs are interconnected by means of X2 interfaces and to the MME/GW entity by means of and S1 interface, as is shown in the figure bellow. The S1 interface supports a multicast relationship between MME/GW and eNBs [17].

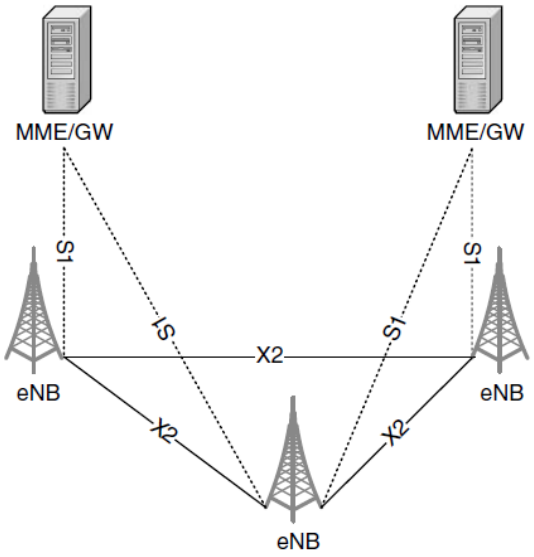

Figure 17 - Network Architecture [4]

In the following sub-chapters we will review the high-level architecture of the evolved packet system (EPS). There are three main components, namely the User Equipment (UE), the Evolved UMTS Terrestrial Radio Access Network (E-UTRAN) and the Evolved Packet Core (EPC). The EPC communicates with packet data networks in the outside world, such as the internet, private corporate networks or the IP multimedia subsystem.

4.1.1. User Equipment

The User Equipment architecture used on the LTE system is identical to the one used by UMTS and GSM. The mobile equipment can be divided into two components, namely the Mobile Termination (MT), which handles all the communication functions, and the Terminal Equipment (TE), which terminates the data streams.

4.1.2. Evolved UMTS Terrestrial Radio Access Network – E-UTRAN

The E-UTRAN handles the radio communications between the mobile (UE) and the evolved packet core (EPC) and is composed by only one element, the evolved Node B. Each eNB is a base station that controls the mobiles in one or more cells. A mobile communicates with just a base station and one cell at a time, so there is no equivalent of the previous generations of cellular systems handover. The base station that is communicating with a mobile is known as its serving eNB.

The eNB has two main functions. The primary one is to send radio transmissions to all its mobiles on the downlink and receive transmissions from them on the uplink, using the analogue and digital signal processing functions of the LTE air interface. The second main function of the eNB is to control the low-level operations of all its mobiles, by sending them signalling messages such as handover commands that relate to those radio transmissions. By performing these functions, the eNB combines the earlier functions of the Node B and the radio network controller, to reduce the latency that arises when the mobile exchanges information with the network.

Each base station is connected to the EPC by means of the S1 interface. It can also be connected by nearby base stations by the X2 interface, which is mainly used for signalling and packet forwarding during handover. The X2 interface is optional, in that the S1 interface can also handle all the functions of X2, albeit indirectly and more slowly. Usually, the S1 and X2 interfaces are not direct physical connections: instead, the information is routed across an underlying IP based transport network.

4.1.3. Evolved Packet Core

One of the few components that have been carried forward from GSM and UMTS to LTE is the EPC's Home Subscriber Server (HSS), which is a central database that contains information about all the network operator's subscribers.

The EPC's point of contact to the outside world (internet, IMS, etc.) is the packet data network (PDN) gateway (P-GW). The P-GW also performs several IP functions such as address allocation, policy enforcement, packet filtering and routing. Each mobile is assigned to a default PDN gateway when it first switches on, to give it always-on connectivity to a default packet data network, but, later on, a mobile may be assigned to one or more additional PDN gateways, if it wishes to connect to additional packet data networks. Each P-GW stays the same throughout the lifetime of the data connection.

The Serving Gateway (S-GW) acts as a router and forwards and receives packets to and from the eNB serving the UE. A typical network might contain a handful of serving gateways, each of which looks after the mobiles in a certain geographical area. Each mobile is assigned to a single serving gateway, but the serving gateway can be changed if the mobile moves sufficiently far.

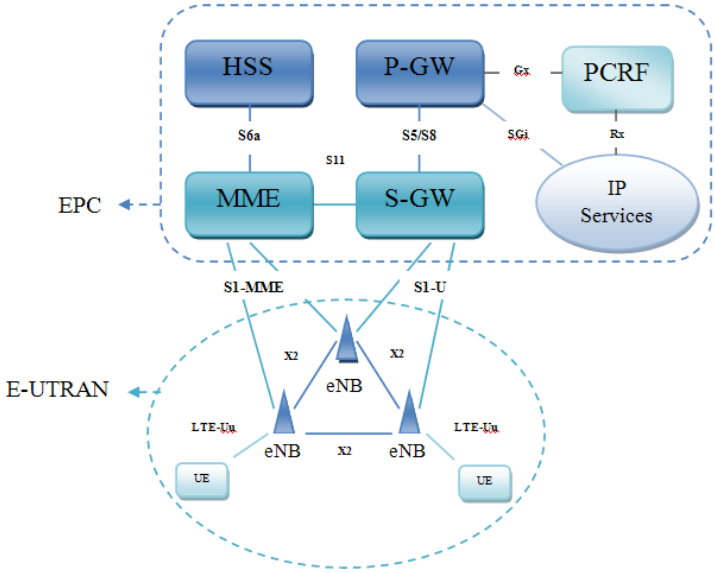

Figure 18 - EPS Architecture

The Mobility Management Entity (MME) is a signalling only entity that controls the high-level operation of the mobile, by sending signalling messages about issues such as security and management of data streams that are unrelated to radio communications. The main duties of MME are idle-mode UE reachability, including the control and execution of paging retransmissions, tracking area list management, roaming, authentication, authorization, P-GW/S-GW selection, bearer management, including dedicated bearer establishment, security negotiations and NAS signalling, etc. An advantage of a separate network entity for signalling is that the network capacity for signalling and traffic can grow independently.

4.1.4. Roaming

Each operator has a Public Land Mobile Network (PLMN) and users move between those PLMNs when moving between countries. After changing the PLMN they connect to the E-UTRAN, MME and S-GW of the visited LTE network. One of the important roaming features of LTE is the ability to use the home network P-GW to be used allowing the user to access the home network services in a visited network.

4.2. Physical Layer

LTE radio access consists of four protocol layers: PHY (physical layer), MAC (Media Access Control layer), Radio Link Control (RLC) and Packet Data Convergence Protocol (PDCP). The PHY and MAC layers utilize transport blocks to exchange information. At the PHY layer, several channels are allocated for data and control communications.

LTEs physical layer supports multiple users in the downlink using OFDM and multiple accesses in the uplink using SC-FDMA (Single Carrier Frequency Division Multiple Access). However, although OFDM is a multicarrier scheme, SC-FDMA is a single-carrier channel access scheme that provides the advantage of a low Peak-to-Average-Power Ratio (PAPR). The 8th Release of LTE also supports scalable bandwidth up to 20 MHz, and uses Downlink/Uplink frequency selective and Downlink frequency diverse scheduling [18].

4.2.1. Frame Structure

The frame structure defines frame, subframe, slot and symbol duration in the time domain. LTE operates either using FDD (Frequency Division Duplexing) or TDD (Time Division Duplexing) and the radio frames are common to both these procedures and 10ms long.

4.2.1.1. FDD Frame Structure

In FDD, each frame consists of ten 1ms-subframes. Each subframe, in both FDD and TDD, has two slots of 0.5ms each (7 OFDM symbols for normal cyclic prefix) with reference symbols located within each slot [19]. Download control signalling is located in the first *n* OFMD symbols (*n* ≤ *3*), where *n* can be dynamically changed every subframe, followed by data transmission.

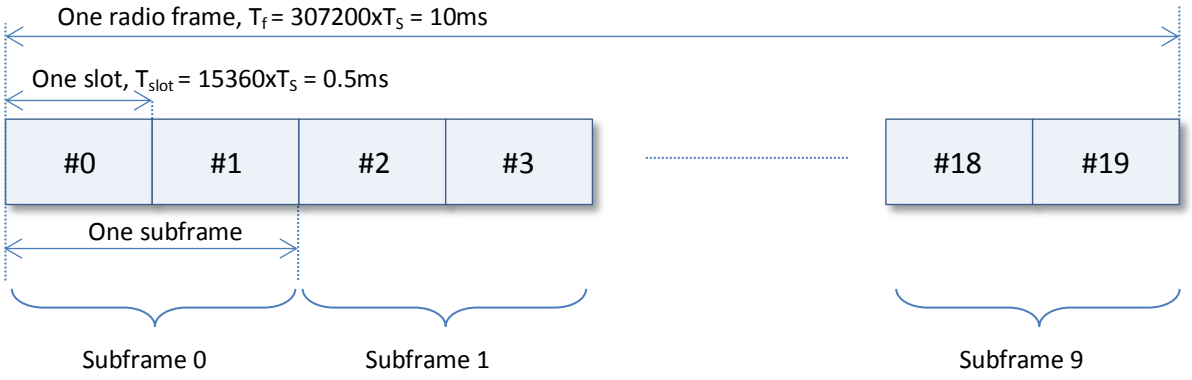

Figure 19 - FDD frame structure

4.2.1.2. TDD Frame Structure

In TDD LTE uses two 5ms half-frames, which are then further divided into 4 subframes and one special subframe, based on the downlink-to-uplink switch point periodicity. TDD frame structure can then be configured into seven different formats of 1ms-subframes.

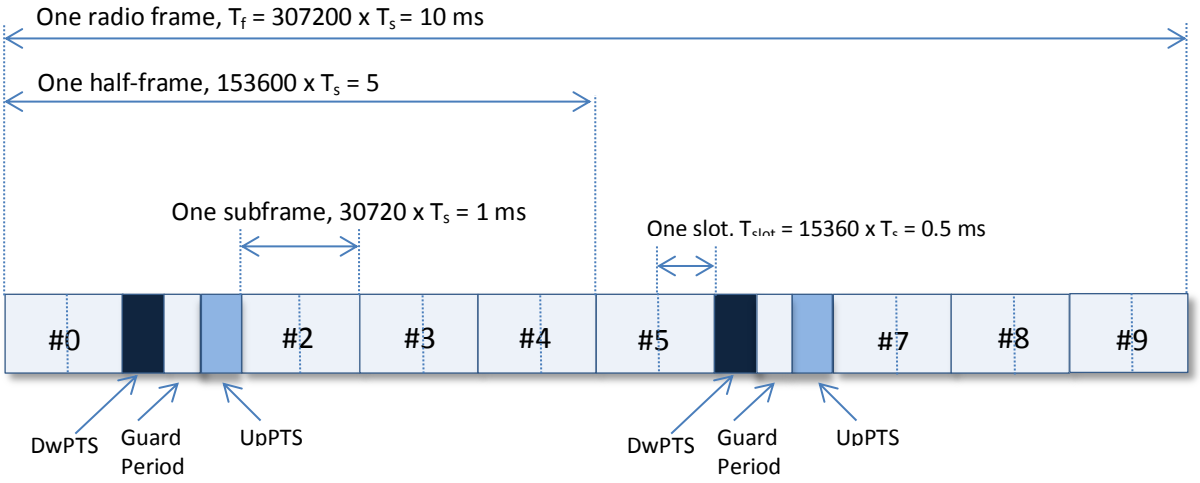

Figure 20 - TDD frame structure

Subframe #1 and sometimes subframe #6 consists of three special fields: Downlink Pilot Timeslot (DwPTS), Guard Period (GP) and Uplink Pilot Timeslot (UpPTS) [4]. The duration of these special fields varies according to the different formats available. The rest of the subframes in the radio frame can be either reserved for uplink transmissions or downlink transmissions, again, according to the type of format.

This kind of flexibility on the slot downlink or uplink direction assignment in a frame enables asymmetric data rates. Depending on the switch point periodicity, there can be one or two changes of direction within the frame, providing considerable deployment flexibility.

4.2.2. Resource Element and Resource Block

PHY resource allocation is organized in units of resource blocks (RB). Each resource block is a rectangular structure containing resource elements (RE), or subcarriers, of the same modulation types. So, a RE occupies one OFDM or SC-FDMA symbol in the time domain and one subcarrier in the frequency domain. A list of possible RB configurations is displayed on the table below; being the most commonly used seven symbols by twelve subcarriers per RB.

Table 2 - Resource Block Configuration

	Normal Cyclic Prefix	Extended Cyclic Prefix	
	Subcarrier Spacing: 15kHz	Subcarrier Spacing: 15kHz	Subcarrier Spacing: 7.5kHz
Downlink	7x12	6x12	3x24
Uplink	7x12	6x12	-

Each of the two slots per subframe equals one RB wide in the time domain and contains between 6 and 110 RBs for 1.4MHz to 20MHz channel bandwidth, respectively, in the frequency domain.

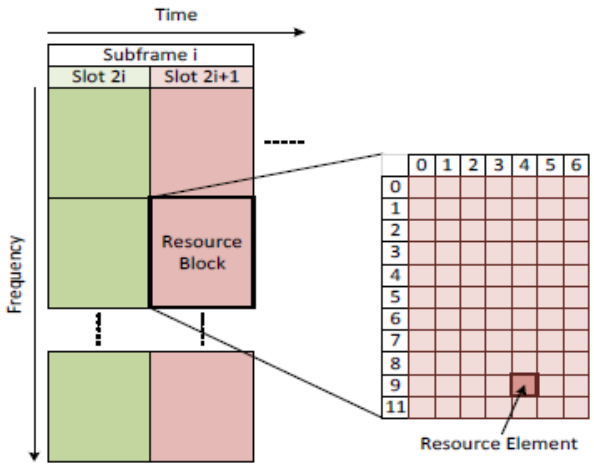

Figure 21 - Resource Block Structure

4.2.3. Physical Channels

The different PHY channels of LTE, as well as reference signals, are then mapped onto this structure of resource elements. The following channels provide Downlink control signalling: physical control format indicator channel (PCFICH), physical hybrid automatic repeat request (HARQ) indicator channel (PHICH), and physical Downlink control channel (PDCCH). Table 3 provides a brief overview of the purpose of these control channels.

The Downlink and Uplink scheduling assignment transmitted on the PDCCH is addressed to a specific user, and contains control information needed for data reception and demodulation. Users are assigned data allocation in quanta of RBs, where and RB is defined as 12 REs by one slot [18].

In the Uplink, SC-FDMA is implemented via discrete Fourier transform spread OFDM (DFT-S-OFDM), with similar numerology to the OFDM transmission scheme used on the Downlink, with the main difference being that the constellation symbols are DFT precoded before mapping to the different subcarriers. The DFT precoding operation is performed to reduce the cubic metric (CM) of the signal, leading to higher maximum transmit power [20]. This CM reduction may be used to improve cell

edge coverage and conserve UE battery life. Like what happened in the downlink, the frequency domain orthogonality is maintained among intra-cell users, which allows the eNBs to efficiently manage the amount of interference seen at the base stations.

Table 3 - Physical Channels on LTE

Channel		Purpose
DL	Physical Shared Channel (PDSCH)	Carrier user data (DL)
	Physical broadcast channel (PBCH)	Carry broadcast information
	Physical multicast channel (PMCH)	Carry multicast services
	Physical Control Format Indicator (PCFICH)	Indicate the size of the control region in number of OFDM symbols
	PHICH	Carry ACK/NACK associated with UL transmission
	PDCCH	Carry DL scheduling assignments and UL scheduling grants
UL	Physical Shared Channel (PUSCH)	Carry user data (UL)
	Physical Uplink Control (PUCCH)	Carry ACK/NACK associated with DL transmission, scheduling request, and feedback of DL channel quality and precoding vector
	Physical random access channel (PRACH)	Carry random access transmission

5. LTE Advanced

The International Telecommunication Union (ITU) set a list of requirements for the fourth generation (4G) of cellular communications, under the name of IMT-Advanced, setting a peak data rate of at least 600Mbps on the downlink and 270Mbps on the uplink, in a bandwidth of 40MHz. It's clear that the LTE system didn't fulfil those requirements.

Driven by ITU's requirements, 3GPP started studying how to enhance the capabilities of LTE. The result of such studies was a specification for a system known as LTE-Advanced or the LTE's Release 10, with the following main requirements: peak data rate of 1Gbps in the downlink, and 500Mbps in the uplink. In practice, the system has been designed so that it can eventually deliver a peak data rate of 3 and 1,5Gbps respectively, using a total bandwidth of 100MHz, made from five different separate components of 20MHz each.

The specifications also include goals for the spectrum efficiency and the capacity of being compatible with other cellular systems. These goals are possible due to the use of some enabling technologies, such as carrier aggregation, relaying, enhancements to multiple antenna transmissions on both the uplink and the downlink and multi-point coordination/cooperation. Since the aim of this thesis is study coordination techniques, we present in more detail the last enabling technology, the first three are briefly discussed.

5.1. Carrier Aggregation

In order to support a maximum bandwidth of 100MHz, LTE-Advanced allows a mobile to transmit and receive on up to five component carriers (CCs), each of which has a maximum bandwidth of 20MHz. This technique is known as Carrier Aggregation [2]. Carrier Aggregation enables peak data rates in excess of 1Gb/s in the downlink and 500 Mb/s in the uplink [18].

There are three scenarios in which Carrier Aggregation can happen. The first one, designated by inter-band aggregation, the component carriers are located in different frequency bands, thus, the mobile may require different radio components to support each band and the cell's coverage are in each band may be very different. The component carriers are separated by a multiple of 100 kHz, which is the usual LTE carrier spacing.

The second scenario is called Non-contiguous intra-band aggregation, and is characterized by having the component carriers in the same band. This scheme deals with the same problems noted in the first scenario, and simplifies the design of the mobile and network.

In Inter-band aggregation, the last scenario, the component carriers are in the same band and are adjacent to each other. They are separated by a multiple of 300 kHz, which is consistent with the orthogonality requirements, so that the set of sub-carriers are orthogonal to each other and do not interfere.

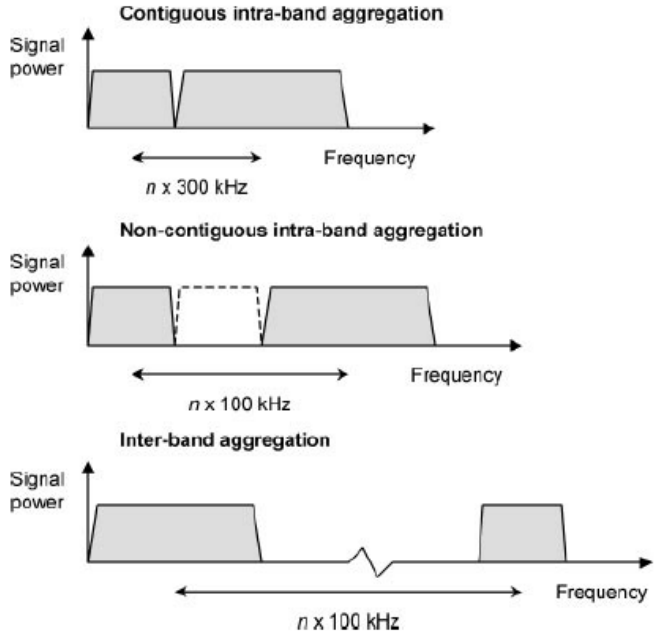

Figure 22 - Carrier Aggregation Scenarios [3]

In FDD mode the allocations on the uplink and downlink can be different, but the number of downlink component carriers is always greater than or equal to the number used on the uplink. In TDD mode, each component carrier uses the same TDD configuration, so it allocates its subframes to the uplink and downlink in the same way.

5.2. MIMO Enhancements for LTE-Advanced

Multiple-Input Multiple-Output is an important component in meeting the goals set for LTE-Advanced. This technology allows the possibility of achieving beamforming and spatial multiplexing techniques, which are already playing major roles in LTE. Enhancements of MIMO technologies for LTE-Advanced are driven by the need to increase the peak data rates, improving the system performance and supporting various transmissions schemes with a universal structure.

In LTE-Advanced it is introduced the support for dual layer beamforming, in which the base station transmits to two receive antennas that are located on one or two mobiles. This technique is extended as a part of LTE Release 10 (LTE-Advanced), by providing full support for downlink multiple users MIMO and by increasing the maximum number of base stations antenna ports to eight. There are then possibilities to support antenna configurations of 8x8 on the Downlink and 4x4 on the Uplink.

This same technique can be used to support single user MIMO, with a maximum of eight antenna ports and eight transmission layers, being a preferred scenario in uncorrelated channel conditions or to maximize the peak data rate of a single mobile, while multiuser MIMO is preferred in correlated channel conditions or to maximize the cell capacity.

The LTE-Advanced downlink spatial multiplexing is enhanced to support up to eight transmission layers with an enhanced reference-signal structure for demodulation. Additionally, feedback of CSI is based on a separate set of reference signals – CSI reference signals. While UE-specific reference signals are denser in frequency but only transmitted when data is transmitted on the corresponding layer, CSI reference signals are relatively sparse in frequency and time, but regularly transmitted from all antennas at the base station. Separating these two types of reference signals helps reducing the reference signal overhead, especially for high degrees of spatial multiplexing, and allows for implementation of various beam-forming schemes.

In the Uplink, Release 10 set spatial multiplexing of up to four layers. The basis is a codebook-based scheme where the scheduler in the base station determines the precoding matrix applied in the UE. The selected precoding matrix is then applied to the uplink data transmission as well as the uplink demodulation reference signals. The reference signals are enhanced to support up to four antennas.

5.3. Relaying and Repeaters

The use of Relay Nodes (RN) opens up new possibilities for increasing the density of the deployed infrastructure, with the aim of cutting the distance between transmitters and receivers thus allowing higher data rates, improving group mobility, cell edge coverage as well as extends coverage to heavily shadowed areas or areas beyond the cell range. Another potential benefit of this scheme is to cut back on CAPEX and OPEX by having cells of relatively larger sizes. Repeaters, which are already being used today for dealing with coverage holes, also play a key role by simply amplifying and forwarding the received analogue signals, so it appears to the receiver as an extra source of multipath. Unfortunately the repeater also amplifies the incoming noise and interference as well as the received signal, which ultimately limits its performance.

A relay takes things a step further, by decoding the received radio signal, before re-encoding and rebroadcasting it. By doing this, it removes the noise and interference from the retransmitted signal, so it can achieve a higher performance than a repeater. In a typical relay network scenario, the Relay Nodes are connected through a donor cell to the radio access network. Relays can be divided in three categories:

- **Layer 1 (L1)** Relay, also known as Amplify-and-Forward Relay is easy to implement through RF amplification with relatively low latency. It is not very practical, as undesired noise is also amplified with the desired signal.

- **Layer 2 (L2)** Relay carries out decode-and-forward operations, with more autonomy to achieve performance optimization. To do so, a significant amount of delay is introduced to the system, as an intermediate node decodes and re-encodes received data. However, no noise is forwarded by this kind relay node.
- **Layer 3 (L3)** Relay, also referred to as Self-Backhauling, is very similar to L2 but the self-backhauling solution has much less impact on the eNB design and does not require any new nodes, protocols or interfaces to be standardized as the existing solutions are reused and may be preferable over the L2 counterpart. On the other hand, L3 may cause more overhead than L2.

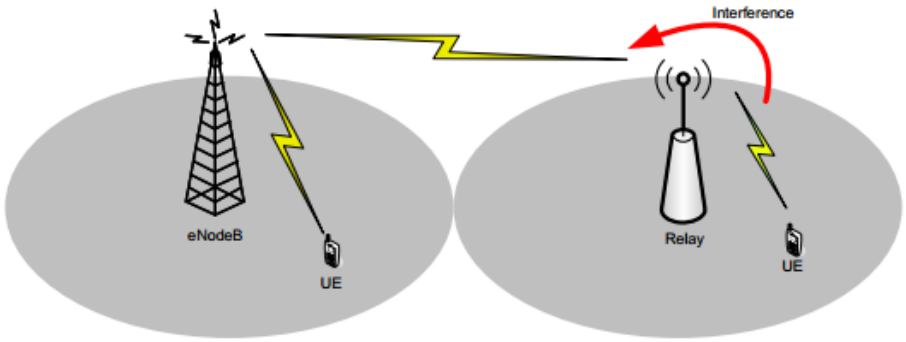

Figure 23 - Deployment of a relay [20]

Current 3GPP considerations are focused on single hop relays with the self-backhauling as main candidate [21].

Relays under consideration by the 3GPP can also be classified as transparent or non-transparent, from the point of view of the user equipment. In transparent relay, the UE is not aware that it is communicating with the eNB via a relay, used to achieve throughput enhancement of UEs located within coverage of the eNB with less latency and complexity. In non-transparent relays, the UE is aware of its communication with an eNB through a relay. In this case, the data traffic and control signal transmissions between the user terminal and the eNB are forwarded along the same relay path. This method may not be an efficient way for all scenarios, because both data and control signalling are conveyed multiple times over the relay links and the access link of a relay path.

From the relay architecture point of view, LTE-Advanced defines two types of connections between the relay node and eNB, namely inband and outband. In the case of inband connections, the eNB-RN link share the same band with direct eNB-to-UE. For outband connections, the eNB-RN link does not operate in the same band as eNB-UE. To enable the inband communications, LTE-Advanced defines resources subdividing procedures, where network resources are reserved for the eNB-RN link and cannot be used by the access link.

5.4. Coordinated Multi-Point Transmission – CoMP

The biggest setback in designing a cellular communication system is the effects of the signals power fading and interference. While fading reduces the quality of a wireless connection between a base station and a mobile device, interference restricts the reusability of the spectral resource in space, thus limiting the overall spectral efficiency.

The current cellular systems are mainly limited by inter-cell interference, especially in urban areas, where the rate demands is larger and hence the number of base stations deployed is larger. Since the Release 8 of LTE already uses techniques that can unsure a high level of spectral efficiency, seeing that the only way to increase the signal to noise ratio (SNR) is to decrease the noise (interference) in the system.

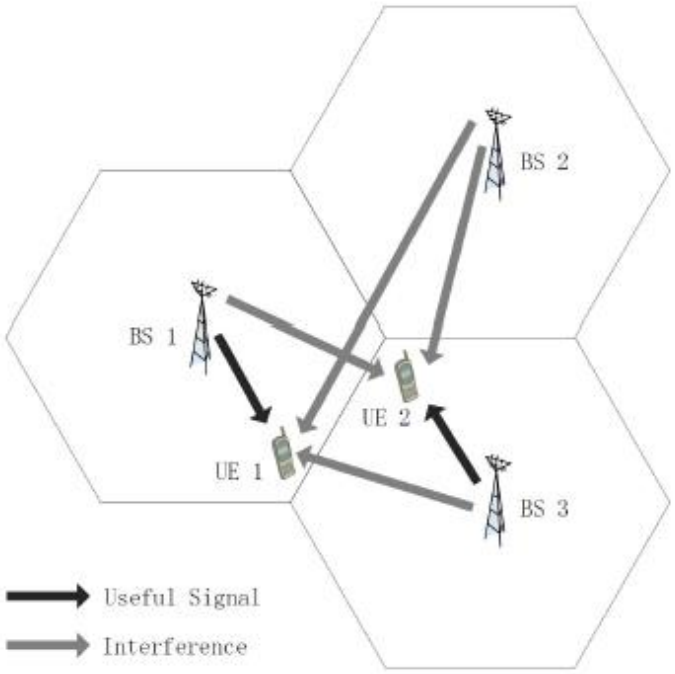

Figure 24 - Conventional Cellular System [21]

One of the most proactive ways of dealing with this interference is the introduction of an interference-aware multi-cell coordination at the base stations side. The principle of said coordination protocols is the following: Base Stations no longer tune separately their physical and link/MAC layer parameters or decode independently of one another, but instead coordinate their coding or decoding operations on the basis of global channel state and user data information exchanged over backhaul links among several cells [22].

One of the issues being addressed beyond Release 10 is Coordinated Multipoint (CoMP) transmission and reception. This term refers to a wide range of different techniques that have in coming the coordination between the radio communications that are taking place in nearby cells. Its aim is to increase the data rate at cell edge and the overall throughput of the cell.

CoMP may refer to a multitude of schemes that have in common that intra- or inter-cell interference is somehow taken into account or even exploited to enhance data rates and/or fairness. CoMP can be applied both in the downlink and the uplink. All schemes come with the cost of increased demand on backhaul (high capacity and low latency), higher complexity, increased synchronization requirements, more channel estimation effort, mover overhead and so on [23].

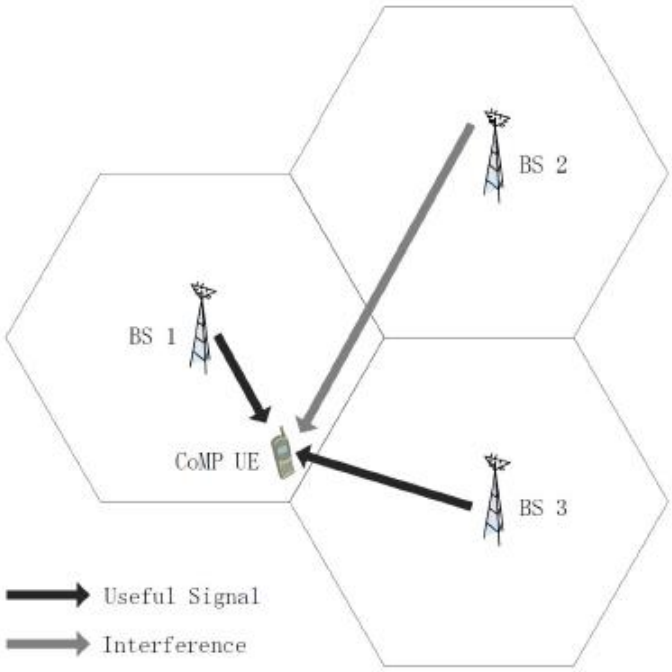

Figure 25 - CoMP cellular System Model [23]

CoMP schemes can be classified according to the extent of cooperation taking place between cells:

- **Non-cooperative, but interference aware transceivers schemes**, where base stations or terminals adjust their transmit or receive strategy according to some knowledge on interference. This does not require explicit information exchange between cells, but the estimation of interference must be enabled through appropriate reference signal design. This class of schemes includes single-cell multi-user signal processing, as used in LTE Release 8 [24].
- **Interference Coordination schemes**, where limited data is exchanged between cells for the purpose of multi-cell cooperative scheduling, multi-cell interference-aware link adaptation, or multi-cell interference-aware precoding.
- **Joint Processing schemes**, were user data to be transmitted is available in multiple sectors of the network. A subclass of joint processing is joint transmission, where the data channel to one terminal is simultaneously transmitted to multiple sectors.

The most important and more used CoMP schemes are Joint Processing and Interference Coordination, and they are going to be discussed in the following sub-chapters, with a focus on the downlink, being that the purpose of this thesis.

5.4.1. Joint Processing

In the class of joint processing/transmission, multiple base stations (or transmission points or cells) jointly transmit signals to the mobile terminal, improve the received signal quality or actively cancel interference from other mobile terminals [25]. So, in this case, there has to be data and channel state information (CSI) shared between different cells to be jointly processed at these cells. As a result of this joint processing, received signals at the intended mobile terminal will be coherently or non-coherently added together. If time-frequency synchronization transmission (TFST) is operated, that is, if the data of a UE is simultaneously transmitted from multiple points on a time-frequency resource to improve the received signal quality and/or data throughput, then Joint Processing (JP) will become Joint Transmission (JT) [26]. The effect of Joint Processing largely depends on the application of the Precoding method in the transmission points [27].

Joint Transmission can be achieved by codebook-based precoding, to reduce feedback signal overhead [28]. In principle, the best precoding matrixes for inter-cell site coordination are selected in addition to the individual selection of the best precoding matrix at each cell site so that the received signal-to-interference-plus-noise power ratio (SINR) is maximized at a UE set among the predetermined precoding matrix candidates. Other implementation methods can be performed in order to achieve the principle operation.

The cost for the existing coordination schemes with joint processing is the heavy exchange of channel state information and signal information over backhaul links.

The design of efficient algorithms and principles that could reduce these complex feedback requirements demands solutions that restrict the use of joint processing techniques to a limited number of BS or areas of the system. Thus being so, the network is divided into clusters of cells, and the joint processing schemes are implemented within the BSs included in each cluster. The cluster formation can be static, if the cluster remains fixed in time, or dynamic. Within static clusters, three schemes that result in several degrees of joint processing between BSs can be defined [29]:

- **Centralized Joint Processing (CJP):** global Channel State Information (CSI) is available at the transmitter side, and the BSs within the cluster jointly perform the power allocation and the design of the linear precoders.
- **Partial Joint Processing (PJP):** this scheme defines different stages of joint processing between BSs. Joint processing degrees or stages are obtained arranging an active set or subset of BSs for each user in the cluster area. Therefore, a user only receives its data from the subset of BSs included in its active set.
- **Distributed Joint Processing (DJP):** local CSI is available at each BS. Therefore, the power allocation and the precoders are locally calculated at each BS (distributed) but the user may receive its data from several BSs depending on its given channel conditions.

5.4.2. Coordinated Beamforming/Coordinated Scheduling

In this second type of downlink CoMP transmission, commonly designated by CB/CS, a UE data is only available at one transmission point but multipoint CSI is exchanged in the network for interpoint coordination of scheduling and/or beamforming.

The idea of Coordinated Beamforming existed long before the CoMP principle, in the mid-nineties, and mainly targeted the signal-to-interference-plus-noise-ratio (SINR) levelling problem [30], in which the power levels and the beamforming coefficients are calculated to achieve some common SINR in the system or to maximize the minimum SINR. On the other hand, Coordinated Scheduling is a rather recent idea. The first studies mainly divided the entire network in clusters and applied centralized scheduling within each cluster in order to determine which Transmission Point (TP) in the cluster should transmit in each time slot and to which UE [31]. Later studies jointly use CS/CB as a tool to reduce multi-user and multicell interference.

Coordinated beam patterns is a low feedback overhead approach targeting highly loaded cells that consists of coordinating the precoders (beamforming matrices) in the cooperating TPs in a pre-defined manner, in order to reduce interference variation and enable accurate link adaptation, while avoiding spatial CSI feedback from the UE. The TPs, relying on a TP-specific beam pattern in the time-frequency domain, cycle through the fixed set of beams where the cycling period is decided by a central controller and conveyed to the TPs. Based on reports of the best resources and associated channel quality in each cycling period, the UE can be scheduled in the subframes or sub-bands where the coordinated beams provide the best channel conditions.

Precoding Matrix Indicator coordination mitigates the inter-TP interference based on the report of a restricted or recommended PMI, measured by the terminals [23], which corresponds to potential precoders at an interfering TP. Assuming that the UE and base stations have knowledge of a codebook composed of quantized precoders, PMI restrictions and PMI recommendation techniques constrain the interfering TPs to use only those precoders that belong to a subset of the codebook in order to enhance cell edge performance. When there's a PMI restriction, the cell edge users calculates and reports to their serving cell the restricted PMIs, defined as the PMIs that create the highest interference if used as a precoders in the interfering TPs. The opposite is true to the case of a PMI recommendation, which is defined as the PMIs that create the lowest interference if used as precoders in the interfering TPs.

Interference suppression-based coordinated beamforming refers to a coordinated selection of the transmit precoders in each TP that aims at eliminating or reducing the effect of inter-TP interference. The Base Stations compute a new transmit filter based on the CSI feedback from the serving and interfering TPs, relying typically on zero-forcing beamforming (ZFBF), which is designed by forcing the interference from a reference TP to UEs served by other TPs to zero, joint leakage suppression (JLS) criteria that maximizes the signal-to-leakage-plus-noise ratio (SLNR) to the UE served by the reference TP, and others. Interference-suppression-based CB provides more design flexibility than PMI coordination, but is more demanding in terms of complexity, CSI accuracy, feedback overhead, backhaul overhead, and scheduling coordination.

5.4.3. Clustering

CoMP schemes, as seen in the previous sections, require additional signalling overhead on the air interface and the backhaul network. Consequently, in practical applications, only a limited number of base stations can cooperate, in order to keep the overhead manageable. So, this cooperative base stations form a cooperating cell cluster, set up adaptively based on RF channel measurements and UE positions, in order to exploit the advantages of CoMP efficiently at limited complexity.

A key requirement for adaptive cluster algorithms in CoMP schemes is that it fits into the LTEs' architecture of the radio access and/or core network. The 3GPP standard already supports a framework for self-organization networks (SONs), in order to maintain automatic configuration and optimization of the network [23].

One of the most central questions in practical CoMP schemes is how small cell clusters can be formed, within which CoMP can be used at reasonable overhead and complexity, but still providing major portions of the potential CoMP gain. Two clustering schemes can be defines, regarding the previous stated matters: static clustering, where clustering is only performed once, based on either field measurements or ray-launching simulations of concrete deployments [32], and then fixed, and dynamic clustering, where UE-centric measurements are used to adapt clustering decisions over time to traffic demand and UE locations [33].

5.4.4. Backhaul for CoMP

CoMP techniques need to exchange direct information between Base Station, with different requirements of the necessary backhaul throughput and latency, depending on the type of CoMP approach at stake.

MIMO cooperation requires the sharing of both channel state information and user data. In determined CoMP schemes, the data symbols of all users must be known at all cooperating bases. In a system where a cluster composed of L base stations cooperate among each other, data is sent to the these base stations results on a factor of L increase in the backhaul bandwidth [22]. Compared with the exchange of data, the bandwidth required for exchanging channel state information is very small, for the case of moderate mobile speeds. These bandwidth requirements for the exchange of CSI increase for higher mobile speeds and more frequency selective channels.

As an alternative to sending the data signals and CSI to the base stations as it is, one could send a quantized signal of this information, in order to reduce the backhaul requirements of a CoMP system. A study of this technique will be conducted in the next chapter, and its benefits will be discussed.

For connectivity between sites, the logical X2 interface could be used, being either a direct physical link or a multihop link, depending on the network's backhaul architecture. The delay depends on the network topology, network node processing delay and line delay [23].

The backhaul network for CoMP systems has to take in to account latency requirements, and seeing that CoMP is integrated with the hybrid automatic repeat request (HARQ)

process, the backhaul latency will be limited by said process. Another impact of backhaul latency is that the exchanged channel information is outdated.

6. Cooperative Schemes Implemented

In the previous chapters we discussed the influence of the intercell interference in limiting the cellular system capacity and how multicell cooperation is a promising solution for cellular systems to mitigate these effects. This technology, under study in LTE-Advanced, was discussed in Chapter 5, under the coordinated multipoint (CoMP) concept.

Previously we noted there were two main types of CoMP based techniques, depending on the amount of information shared by the transmitters through the backhaul network, namely Coordinated Beamforming/Scheduling (CB/CS) and Joint Processing (JP). These techniques can also be characterized by where the processing takes place, i.e., centralized if the processing takes place at a central unit (CU) or distributed if it takes place at the different transmitters.

Coordinated centralized beamforming approaches, where transmitters exchange both data and channel state information (CSI) for joint processing at the CU, promise large spectral efficiency gains than distributed interference coordination techniques, but typically at the price of larger backhaul requirements and more severe synchronization requirements. Two centralized multicell precoding schemes based on the waterfilling technique have been proposed in [34]. It was shown that these techniques achieve a performance, in terms of weighted sum rate, very close to the optimal. In [35] a clustered BS coordination is enabled through a multicell block diagonalization (BD) strategy to mitigate the effects of interference in multicell MIMO systems. A new BD cooperative multicell scheme has been proposed in [36], to maximize the weighted sum-rate achievable for all the UTs.

Distributed precoding approaches, where the precoder vectors are computed at each BS in a distributed fashion, have been proposed in [37]. It is assumed that each base station has only knowledge of local CSI and based on that a parameterization of the beamforming vectors used to achieve the outer boundary of the achievable rate region was derived. In [38] , distributed precoding schemes based on zero-forcing criterion with several centralized power allocation based on minimization of signal-to-noise ratio (SINR) have been derived.

In the previous approaches, it was assumed that the transmitters share the entire data of all UTs. However, there are distributed beamforming approaches where the transmitters do not share the data, which fall into the interference channel (IC) framework. The local CSI, i.e., the CSI between a given BS and all UTs, is used by transmitters to design individual precoders to transmit exclusively to the users within their own cell [39], [40]. This approach, known as inter-cell interference nulling (ICIN), in which each BS transmits in the null-space of the interference it is causing to neighbouring cells, has been discussed in the 3GPP LTE-Advanced literature. The authors of [41] proposed a non-iterative distributed solution to design precoding matrices for multicell

systems, which maximizes the sum-rates for only a two-cell system at high SNR. In [42], a coordinated beamforming approach based on the virtual SINR framework, for a special case of two transmitters, has been proposed.

In this work we evaluate coordinated beamforming techniques for the downlink of multicell MISO-OFDM systems. In that matter, distributed precoding approaches, where precoder vectors are computed at each BS and it is assumed that each base station has only knowledge of local CSI, are proposed and assessed. Then the system is further optimized by computing a power allocation algorithm over the subcarriers that minimizes the average BER, under per-BS power constraint. Both, upper and lower bounds, used to reduce the search space for the optimum solution and therefore efficiently perform the power allocation procedure, are derived. Also, we assess the performance of the precoders under imperfect CSI. A quantized version of the CSI associated to the different links between the BS and the user terminal (UT) is feedback from the UT to the BS, and then exchanged by the different BSs. We consider the channel quantization technique discussed in [43]. This information is then employed by the different BSs to perform the precoding design. A new DVSINR precoder explicitly designed under imperfect CSI is proposed. The considered schemes are implemented and evaluated under the LTE parameters and scenarios.

6.1. System Model

The system considered throughout this work is based on the MISO interference channel, where B BSs, each equipped with N_{tb} antennas, transmit to B single antenna UTs, as shown in Figure 26.

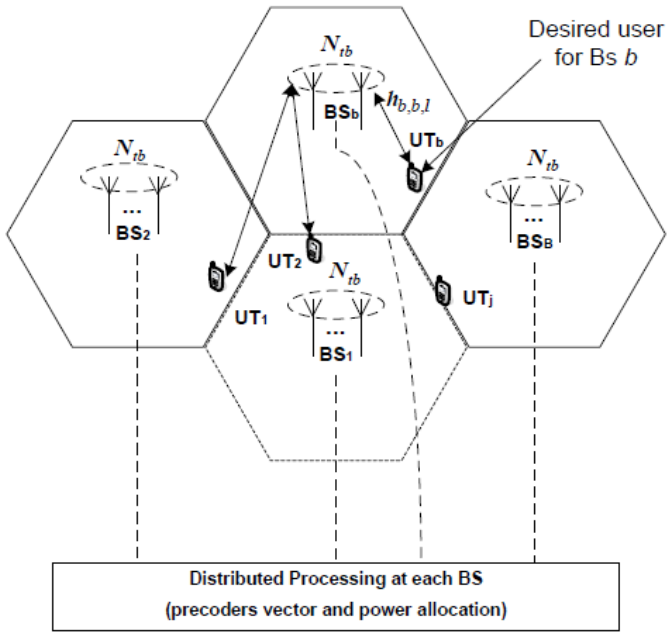

Figure 26 - System Model Considered

It is assumed that we have an OFDM based system with N_C available subcarriers. Under the assumption of linear precoding, the signal transmitted by the BS b on subcarrier l is given by,

$$\mathbf{x}_{\mathrm{b,l}} = \sqrt{p_{b,l}}\mathbf{w}_{\mathrm{b,l}}s_{b,l} \tag{6.1.1}$$

where $p_{b,l}$ represents the transmitted power allocation to subcarrier l at BS b, $\mathbf{w}_{\mathrm{b,l}} \in \mathbb{C}^{N_{tb}\times 1}$ is the precoder at BS b on subcarrier l with unit norm, i.e., $\left\|\mathbf{w}_{\mathrm{b,l}}\right\| = 1,\ b = 1,\dots,B, l = 1,\dots,N_c$. The data symbol $s_{b,l}$, with $\mathrm{E}\left[|s_{b,l}|^2\right] = 1$, is intended for UT b. The average power transmitted at BS b is then given by,

$$\mathrm{E}[\|\mathbf{x}_b\|^2] = \sum_{l=1}^{N_C} p_{b,l} \tag{6.1.2}$$

where $\boldsymbol{x}_b$ is the signal transmitted over the N_c subcarriers.

The received signal at UT b on subcarrier l, $y_{b,l} \in \mathbb{C}^{1\times 1}$, can be expressed by,

$$y_{b,l} = \sum_{j=1}^{B} \sqrt{p_j}\mathbf{h}_{j,b,l}^{H}\mathbf{w}_{j,l}s_{j,l} + n_{b,l} \tag{6.1.3}$$

where $\mathbf{h}_{j,b.l} \sim \mathbb{C}\mathcal{N}(0, \rho_{j,b}\boldsymbol{I}_{N_{tb}})$ of size $N_{tb} \times 1$, represents the channel between user b and BS j on subcarrier l and $\rho_{j,b}$ is the long-term channel gain between BS j and UT b, and $n_{b,l} \sim \mathcal{CN}(0, \sigma^2)$ is the noise.

According to equations (6.1.1) and (6.1.3) the received signal at UT b on subcarrier l can be decomposed in,

$$y_{b,l} = \underbrace{\sqrt{p_{b,l}}\boldsymbol{h}_{b,b,l}^{\boldsymbol{H}}\boldsymbol{w}_{\boldsymbol{b},\boldsymbol{l}}s_{b,l}}_{\textit{Desired Signal}} + \underbrace{\sum_{\substack{j=1\\ j\neq b}}^{B} \sqrt{p_{j,l}}\boldsymbol{h}_{j,b,l}^{H}\boldsymbol{w}_{\boldsymbol{j},\boldsymbol{l}}s_{j,l}}_{\textit{Multiuser Multicell Interference}} + \underbrace{n_{b,l}}_{\textit{Noise}} \tag{6.1.4}$$

and from (6.1.4) the instantaneous SINR of user b on subcarrier l can be written as ,

$$SINR_{b,l} = \frac{\left|\sqrt{p_{b,l}}\boldsymbol{h}_{b,b,l}^{H}\,\boldsymbol{w}_{b,l}^{(type)}\right|^2}{\sum_{\substack{j=1\\ j\neq b}}^{B}\left|\sqrt{p_{j,l}}\boldsymbol{h}_{j,b,l}^{H}\,\boldsymbol{w}_{j,l}^{(type)}\right|^2 + \sigma^2} \tag{6.1.5}$$

where type $= \{\text{DZF}, \text{DVSINR}\}$. Assuming M-arry QAM constellation, the instantaneous probability of error for user b and data symbol transmitted on subcarrier l is given by,

$$P_{e,b,l} = \psi Q(\sqrt{\beta SINR_{b,l}}) \tag{6.1.6}$$

where $Q(x) = (1/\sqrt{2\pi}) \int_x^\infty e^{-(t^2/2)} dt$, $\beta = 3/(M-1)$ and $\psi = (4/log_2 M)(1 - 1/\sqrt{M})$.

6.2. Distributed Precoder Vectors: DFZ and DVSINR

In this chapter, distributed precoding approaches, where the precoder vectors are computed at each BS in a distributed manner, are implemented. These individual precoders, designed at the transmitters, to transmit exclusively to the users within its cell, use only CSI between a given BS and all UTs. This type of design approach is known as inter-cell interference nulling (ICIN), in which each BS transmit in the null-space of the interference.

To design the distributed precoder vectors we assume that the BSs have only knowledge of local CSI and its own data symbols, i.e., BS b knows the instantaneous channel vectors $\mathbf{h}_{b,j,l}, \forall j, l$, and only the data symbols $s_{b,l},\ l = 1, \dots, N_C$ reducing the feedback load over the backhaul network, as compared with the data and/or CSI sharing beamforming approaches.

The precoder vectors used in this chapter were computed based on the distributed zero-forcing (DZF) and distributed virtual signal-to-interference noise ratio (DVSINR).

6.2.1. Distributed Zero Forcing

Zero forcing is considered a classic beamforming strategy which removes the co-terminal interference. A distributed ZF transmission scheme is derived, with the phase of the received signal at each UT aligned. In this case, $\boldsymbol{w}_{b,l}^{(DZF)}$ in equation (6.1.5) is a unit-norm zero forcing orthogonal to $B-1$ channel vectors $\left\{\mathbf{h}_{b,j,l}^{\boldsymbol{H}}\right\}_{j \neq b}$. By using such precoding vectors, the multicell interference is canceled and the data symbol at each BS, on each subcarrier is only transmitted to its intended UT. The SVD of $\left\{\mathbf{h}_{b,j,l}^{\boldsymbol{H}}\right\}_{j \neq b}$ can be portioned as follows,

$$\left\{\mathbf{h}_{b,j,l}^{H}\right\}_{j \neq b} = \mathbf{U}_{b,l} \boldsymbol{\Omega}_{b,l} [\ddot{\mathbf{W}}_{b,l}\ \overline{\mathbf{W}}_{b,l}] \tag{6.2.1}$$

where $\overline{\mathbf{W}}_{b,l} \in \mathbb{C}^{N_{tb} \times (N_{tb}-B+1)}$ holds the $(N_{tb}-B+1)$ singular vectors in the null space of $\left\{\mathbf{h}_{b,j,l}^{H}\right\}_{j \neq b}$. The columns of $\overline{\mathbf{W}}_{b,l}$ are candidates for b's precoding vector since they will produce zero interference at the other UTs. It can then be shown that an optimal linear combination of these vectors can be given by,

$$\boldsymbol{w}_{b,l}^{(DZF)} = \overline{\boldsymbol{W}}_{b,l} \frac{\left(\boldsymbol{h}_{b,b,l}^{H} \overline{\boldsymbol{W}}_{b,l}\right)^{\boldsymbol{H}}}{\left\| \boldsymbol{h}_{b,b,l}^{H} \overline{\boldsymbol{W}}_{b,l} \right\|} \tag{6.2.2}$$

Also, it can be shown that $\mathbf{h}_{b,b,l}^{H} \mathbf{w}_{b,l}^{(DZF)} \sim \chi^2_{2(N_{tb}-K+1)}$.

6.2.2. Distributed Virtual SINR (DVSINR)

While ZF has good performance at high SNR or as the number of antennas increase, the maximal ratio combining (MRT) is the asymptotically optimal solution at low SNR. The optimal strategy lies between these two precoders and cannot be determined without global CSI. However, inspired by the uplink-downlink duality for broadcast channels, there has been derived a novel distributed virtual SINR precoder. The precoder vectors are achieved by maximizing the SINR-like expression in (6.2.3) where the signal power that BS b generates at UT b is balanced against the noise and interference power generated at all other UTs. It was named DVSINR as it originates from the dual virtual uplink and does not directly represent the SINR of any links in the downlink

$$\mathbf{w}_{b,l}^{(DVSINR)} = arg \max_{\|\mathbf{w}\|^2=1} \frac{\left|\mathbf{h}_{b,b,l}^H \mathbf{w}\right|^2}{\sum_{j\neq b}\left|\mathbf{h}_{b,j,l}^H \mathbf{w}\right| + \frac{\sigma^2}{P_{tb}}} \tag{6.2.3}$$

where P_{tb} is the per-BS power constraint. The solution to (6.2.3) is not unique, since the virtual SINR is unaffected by the phase shits in $\mathbf{w}$**.** One possible solution can be written as,

$$\mathbf{w}_{b,l}^{(DVSINR)} = \frac{\mathbf{C}_{b,l}^{-1}\mathbf{h}_{b,b,l}}{\left\|\mathbf{C}_{b,l}^{-1}\mathbf{h}_{b,b,l}\right\|} \tag{6.2.4}$$

where

$$\mathbf{C}_{b,l} = \frac{\sigma^2}{P_{tb}}\mathbf{I}_{N_{tb}} + \sum_{j\neq l}\mathbf{h}_{b,j,l}\mathbf{h}_{b,j,l}^H \tag{6.2.5}$$

6.2.3. Robust DVSINR

In this section, we propose a robust DVSINR algorithm, where the expression (6.2.3) is explicitly minimized under channel quantization errors. The quantization method will be discussed later. The overall channel frequency domain matrix, under quantization errors, can be modeled as $\mathbf{h}_{b,b,l}^Q = \mathbf{h}_{b,b,l} + \mathbf{e}_{b,b,l}$, where $\mathbf{h}_{b,b,l}^Q$ represents the overall quantized channel vector and $\mathbf{e}_{b,b,l}$ is the overall quantized error matrix. Replacing $\mathbf{h}_{b,b,l}$ by $\mathbf{h}_{b,b,l}^Q - \mathbf{e}_{b,b,l}$ in equation (6.2.3) and after some simplification the robust precoder vector is given by

$$\mathbf{w}_{b,l}^{(R-DVSINR)} = \frac{\mathbf{C}_{b,l}^{-1}\mathbf{h}_{b,b,l}^Q}{\left\|\mathbf{C}_{b,l}^{-1}\mathbf{h}_{b,b,l}^Q\right\|} \tag{6.2.6}$$

where

$$\mathbf{C}_{b,l} = \frac{\sigma^2}{P_{tb}}\mathbf{I}_{N_{tb}} + (K-1)\sigma_e^2\mathbf{I}_{N_{tb}} + \sum_{j\neq l}\mathbf{h}_{b,j,l}\mathbf{h}_{b,j,l}^H \tag{6.2.7}$$

where σ_e^2 is the average power of the channel error.

6.3. Power Allocation

In this section, a distributed power allocation algorithm, based on minimization of the average BER over the available subcarriers discussed in [44], is presented. Based on the solution derived in [34] and the Lambert $W_0(x)$ function, we compute upper and lower bounds to reduce the search for the optimal solution decreasing the overall complexity. The criteria used to design this distributed power allocation lead to a redistribution of powers among subcarriers. To derive the power allocation for both precoders, it is assumed that the interference is negligible at both low and high SNR, even for the VSINR precoder.

The precoder defined previously were specifically designed to make the equivalent channels, given by $h_{b,b,l}^{eq} = \mathbf{h}_{b,b,l}^{H}\mathbf{w}_{b,l}^{(type)}$, positive and real valued. Under the assumption of free interference, the SINR defined previously reduces to,

$$\mathrm{SNR}_{b,l} = \frac{\left|\sqrt{p_{b,l}}h_{b,b,l}^{eq}\right|^2}{\sigma^2} \tag{6.3.1}$$

The above expression can be used to derive distributed power allocation because it only contains the local channel gains at BS b. The average BER can be defined as.

$$P_{av,b} = \frac{\psi}{N_c}\sum_{l=1}^{N_C} Q\left(\sqrt{\beta \mathrm{SNR}_{b,l}}\right) \tag{6.3.2}$$

The power allocation problem at each BS b, with per-BS power constraint, can be formulated as,

$$\min_{\{p_{b,l}\geq 0\}}\left(\frac{\psi}{N_c}\sum_{l=1}^{N_C} Q\left(\sqrt{\beta \mathrm{SNR}_{b,l}}\right)\right) \text{ s.t.} \begin{cases} \sum_{l=1}^{N_C} p_{b,l} \leq P_{tb}, & \forall b \end{cases} \tag{6.3.3}$$

The Lagrangian associated with this problem is given by,

$$L(p_{b,l},\mu) = \frac{\psi}{N_c}\sum_{l=1}^{N_C} Q\left(\sqrt{\beta \mathrm{SNR}_{b,l}}\right) + \mu\left(\sum_{l=1}^{N_C} p_{b,l} - P_{t_b}\right) \tag{6.3.4}$$

where $\mu \geq 0$ is the Lagrange multiplier [45]. Since the objective function is convex in $p_{b,l}$, and the constraint functions are linear, this is a convex optimization problem. Thus, it is necessary and sufficient to solve the Karush-Kuhn-Tucker (KKT) conditions, given by,

$$\begin{cases} \dfrac{\partial L}{\partial p_{b,l}} = \dfrac{-1}{N_C} \dfrac{\psi\beta \dfrac{h_{b,b,l}^{eq}}{\sigma} e^{-\frac{1}{2}\left(\beta \frac{h_{b,b,l}^{eq}}{\sigma}\sqrt{p_{b,l}}\right)^2}}{2\sqrt{2\pi}\sqrt{p_{b,l}}} + \mu = 0 \\ \dfrac{\partial L}{\partial \mu} = \sum_{l=1}^{N_C} p_{b,l} - P_{t_b} = 0 \end{cases} \tag{6.3.5}$$

It can be shown that the powers $p_{b,l}$ as function of the Lagrange multiplier are given by,

$$p_{b,l} = \frac{\sigma^2}{\beta (h_{b,b,l}^{eq})^2} W_0\left(\frac{\psi^2\beta^2 (h_{b,b,l}^{eq})^4}{8\pi\sigma^4 N_C^2 \mu^2}\right) \tag{6.3.6}$$

where W_0 stands for Lambert's W function of index 0 [46]. This function $W_0(x)$ is an increasing function with $W_0(x) = 0, x = 0$ and $W_0(x) > 0, x > 0$. Therefore, μ^2 can be easily determined iteratively to satisfy $\sum_{l=1}^{N_C} p_{b,l} = P_{tb}$, by using the bisection method. For $\bar{\mu}_b = \frac{1}{\mu_b^2}$, a sub-interval in which this root must lie should be provided. It can be shown that the Lamberts $W_0(x)$ function is bounded by:

$$\alpha \log(x) \leq W_0(x) \leq x, \qquad x > 0, \forall\, \alpha \in \left[0, \frac{e}{1+e}\right] \tag{6.3.7}$$

Thus, we can derive a lower bound for the root $\bar{\mu}_b$, given by

$$\bar{\mu}_{b_{LB}} = \frac{P_{t_b}}{\sum_{l=1}^{N_C} \dfrac{\psi^2\beta (h_{b,b,l}^{eq})^2}{8\pi\sigma^2 N_C}} \tag{6.3.8}$$

and, for faster algorithm's convergence, the upper bound should be as close to the lower bound as possible. Being so, α should be chosen as $\frac{e}{1+e}$ and therefore, the upper bound is given by,

$$\bar{\mu}_{b_{UB}} = \mathrm{Exp}\left(\frac{P_{t_b} - \sum_{l=1}^{Nc} \dfrac{\sigma^2}{\beta (h_{b,b,l}^{eq})^2} \alpha \log\left(\dfrac{\psi^2\beta (h_{b,b,l}^{eq})^4}{8\pi\sigma^4 {N_C}^2}\right)}{\sum_{l=1}^{Nc} \dfrac{\sigma^2}{\beta (h_{b,b,l}^{eq})^2} \alpha}\right), \text{with } \alpha = \frac{e}{1+e} \tag{6.3.9}$$

thus, the root $\bar{\mu}_b \in \left[\bar{\mu}_{b_{LB}}\, \bar{\mu}_{b_{UB}}\right]$. This scheme is referred as minimum virtual BER power allocation (*type* MVBER PA).

6.4. Quantization

In this section we introduce channel quantization procedures, in order to diminish the system backhaul necessities. The precoding schemes discussed above are evaluated under this quantization method.

Two types of quantization can be considered: uniform quantization or non-uniform quantization. We focus our study on the first. In both cases the quantized signal can be defined as the sum of the quantized signal with an interference error ε_Q.

$$x_Q = x + \varepsilon_Q \tag{6.4.1}$$

In uniform quantization we define L levels, separated by an uniform step Δ. If the original signal, that we want to quantize, has the power of P_x and a mean value equal to zero, and we take continuous values between $-M$ and M, where M is the maximum level of the original signal, then the step is given by $\Delta = 2M/L$ and the signal is equally spaced in L intervals, $[-x_{L/2}, x_{(L-1)/2}]; \dots; [-x_1, 0]; [0, x_1]; [x_1, x_2]; \dots; [x_{(L-1)/2}, -x_{L/2}]$.

The values of the signal x in each of the previous intervals are quantized to the following levels,

$$q_i = \frac{(x_i - x_{i-1})}{2} = (2i-1)\frac{\Delta}{2}, i = -(L-1), \dots, L-1 \tag{6.4.2}$$

The generic characteristic is represented in the Figure bellow. For the uniform quantization the variance is given by $\sigma_\varepsilon^3 = \frac{\Delta^2}{12}$, where Δ is the amplitude of each quantization level.

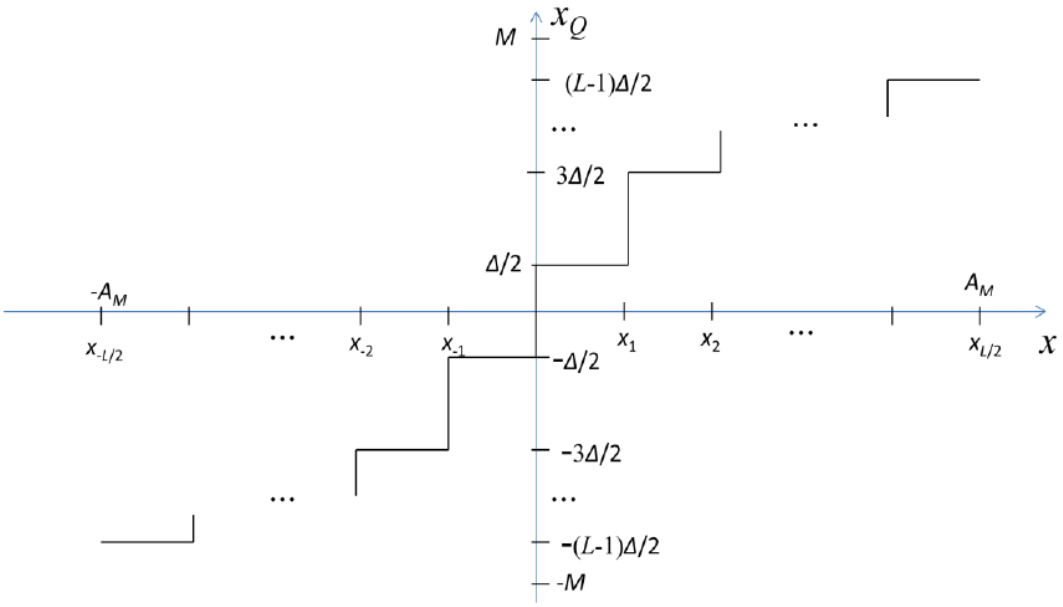

Figure 27 - Characteristic Function for uniform quantization

For input signals whose range is infinity, several authors deduced the optimum step for uniform quantization depending on the signal distributions. In the case of unlimited signal input, the quantization characteristics can be limited between $-A_M$ and A_M, where A_M is the saturation level. In this work we consider ideal clipping, which is given by the expression

$$f_C(x) = \begin{cases} A_M, & x > A_M \\ x, -A_M < x < A_M \\ -A_M, x < -A_M \end{cases} \quad (6.4.3)$$

The signal-to-quantization-noise ratio (SQNR) is given by

$$SQNR = \frac{P_x}{E\left[\left|x - x_Q\right|^2\right]} \quad (6.4.4)$$

which, as we can see, is dependent on the saturation level .

6.4.1. Channel Quantization

The complex baseband representation of the channel impulse response (CIR) can be expressed by

$$h(t,\tau) = \sum_{i=0}^{L_P-1} \beta_i \delta(t - \tau_i) \quad (6.4.5)$$

where L_P is the number of paths, β_i is the complex amplitude of the i^{th} path and τ_i is the delay of the i^{th} path. The power delay profile (PDP) is given by

$$PDP = \sum_i |\beta_i|^2 \delta(t - \tau_i) \quad (6.4.6)$$

Figure 28 show the CIR and frequency response of the channel, where T_U is the duration of the useful symbol, T_{CP} is the cyclic prefix length, which should verify $T_{CP} \geq \tau_{LP-1}$, with τ_{LP-1} being maximum delay, and Δ_f the channel frequency separation between subcarriers.

The frequency response of the time variant channel at time *t* is the Fourier transform of the CIR, considering τ_i is a multiple of sampling interval (T_U/N_C)

$$H(f) = \int_{-\infty}^{+\infty} h(t,\tau) e^{-j2\pi f t} = \sum_{i=0}^{L_P-1} \beta_i e^{-j2\pi f \tau_i} \quad (6.4.7)$$

The overall channel frequency for subcarrier k is then give by,

$$H_k = H(k/T_u) = \sum_i^{L_P-1} \beta_i e^{-j2\pi \frac{k}{T_u} \tau_i} \quad (6.4.8)$$

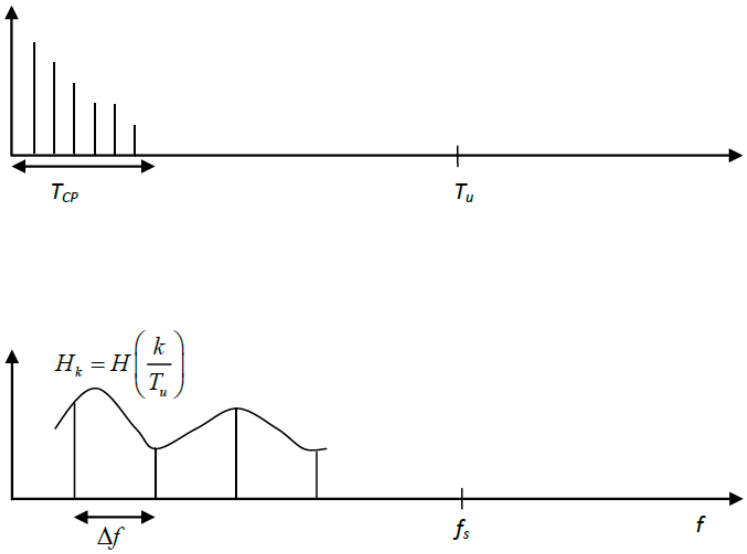

Figure 28 - CIR and frequency response of the channel

Thus, obtaining the N_C frequency values for each subcarrier $\{h_k; k = 0, \dots, N_C - 1\}$. Then, we consider $N_s = N/\Delta$ of these values, obtaining the samples $\{h_{i\Delta}; i = 0, \dots, N_C/\Delta - 1\}$, which we quantize into $\{h_{i\Delta}^Q; i = 0, \dots, N_C/\Delta - 1\}$. Note that we must consider $N_S \geq N_{CP}$, according to the sampling theorem, where $N_{CP} = \frac{T_{CP} N_C}{T_U}$.

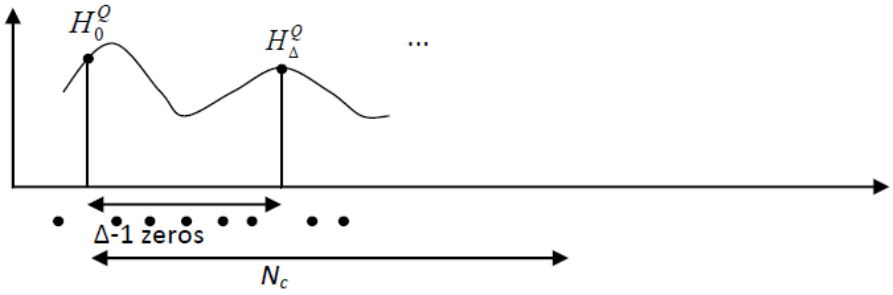

Figure 29 - Frequency Response of the time varying channel

We reconstruct the signal through the IDFT of the quantized samples, obtaining CIR of the reconstructed channel repeated Δ times.

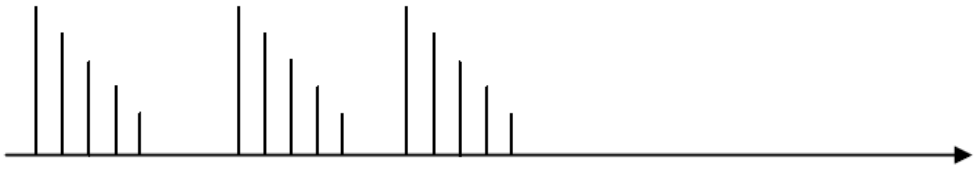

Figure 30 - CIR of the reconstructed channel

By putting zeros in all the taps beyond N_{CP}, we are able to obtain $h(t)$.

Figure 31 - Quantized h(τ)

The reconstructed channel response is finally obtained through DFT of one of the Δ repeated CIRs. Relative distortion is higher for weaker taps, as we can see in the following figure.

The mean square error is given by

$$MSE = \frac{E\left[\sum_k \left|h_k^Q - h_k\right|^2\right]}{E[\sum_k |h_k|^2]} \tag{6.4.8}$$

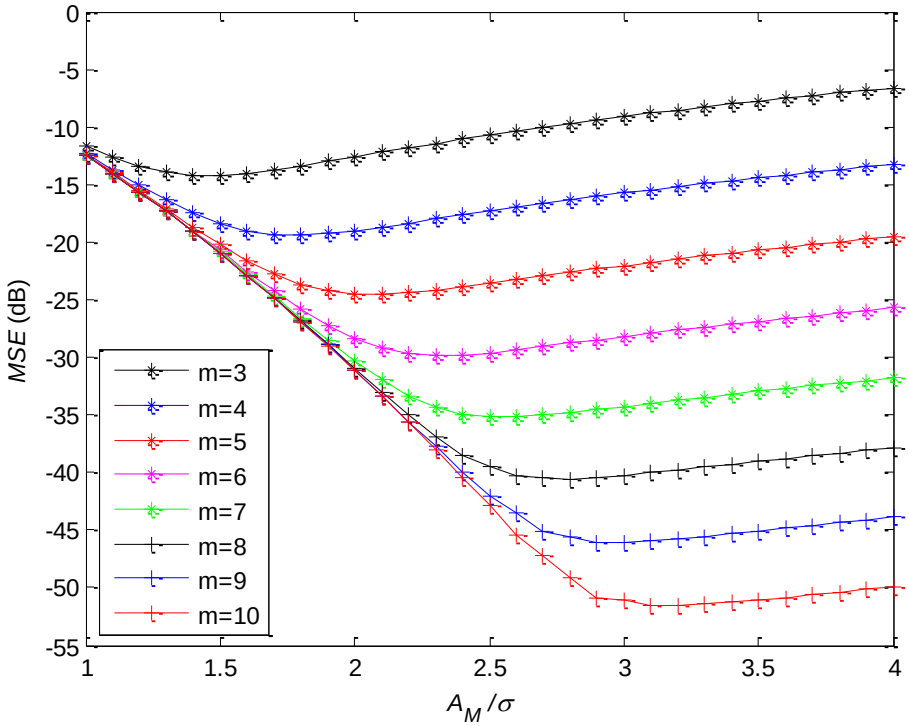

Figure 32 -MSE of channel quantization in function of clipping value, for several numbers of quantization bits and for LTE extended channel model

Figure 32 shows the impact of the normalized saturation level A_M/σ (here σ^2 is the average power of the signal), and the number of quantization bits, m, on MSE. As can be observed, there is an optimum normalized saturation level for each value of m, since the quantizer's saturation becomes too frequent if A_M/σ is small and the quantization interval becomes too high when A_M/σ is high. Hereinafter, we always assume the optimum saturation level for each value of m.

6.5. Channel Coding

In this section we introduce to our system Channel Coding. Data Channel Coding reefers to the process by which both transmitter and receiver of a digital communications system, consuming extra bandwidth by allocating extra bits (used for parity effects), grants more reliability to a connection, protects the digital information from noise and interference and reduces the number of errors.

On LTE, data and control streams from and to the MAC layer are encoded and decoded to offer transport and control services over the radio transmission link. Channel coding schemes are a combination of error detection, error correction, rate matching, interleaving and transport channel or control information mapping onto/splitting channels [47].

Error correction can be considered in two main categories: ARQ (Automatic Repeat Request) and FEC (Forward Error Correction) [48]. With ARQ the receiver requests retransmission of the data packets when errors are detected, and this will be done until the received packets are error-free or a maximum number of retransmissions are achieved. In the FEC category, redundancy bits are added to data bits, making error correction possible. FEC has two main types of codes: block codes and convolution codes. In block codes, the input data blocks, which can be considered as vectors multiplied by a generator matrix, generating a code word vector. Contrarily to block codes, which are memoryless, convolution codes are coding algorithms with memory, which means the coded output bit depends not only on the current bit but also on the *m* previous bits, where *m* is the number of registers in the convolutional encoder.

In LTE both block codes and convolutional codes are used. CRC (Cyclic Redundancy Check), which is a cyclic linear block code, is used for HARQ as an error correction technique [4]. Control channels and data channels in LTE use convolutional and Turbo Codes, respectively, where the last is an enhanced development of convolutional codes achieving near-Shannon performance. Turbo Coding has a fixed coding rate (number of information bits divided by the number of transmitted bits) of $\frac{1}{2}$.

6.5.1. Turbo Coding

Turbo codes, introduced in 1993 by Berrou, Glavieux and Thitimajshima [49], are very powerful codes that can come within a fraction of a dB of the Shannon capacity limit on AWGN (Additive White Gaussian Noise) channels. Turbo codes consist of two main components: a systematic parallel concatenated convolutional code (PCCC), with 8-state constituent encoders, and one Turbo code contention free internal interleaver [4]. The structure of the Turbo encoder used in LTE can be seen in the Figure bellow.

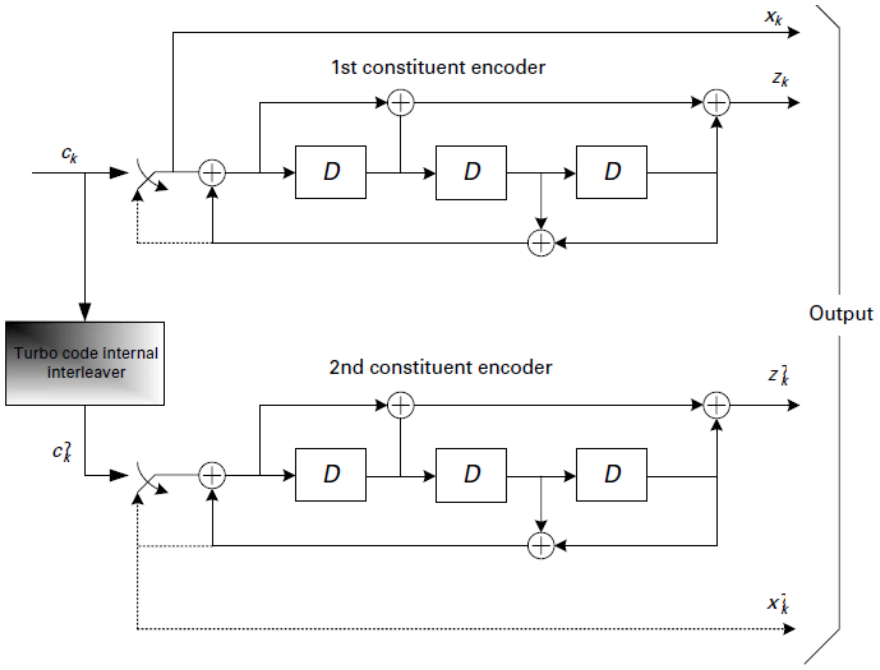

Figure 33 - Structure of the LTE Turbo encoder

After the turbo coding process, there's a second stage of processing, called rate matching, where some of the coded bits are selected for transmission, while the others are discharged, in a process named as puncturing. The receiver has a copy of the puncturing algorithm, so it can insert dummy bits at the points where information was discharged. It can then pass the result through a turbo decoder for error corrections [2].

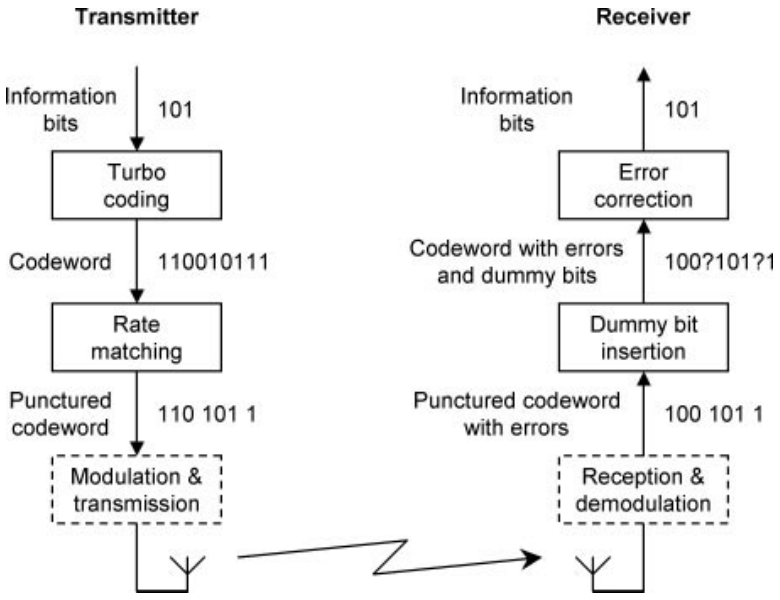

Figure 34 - Block diagram of a transmitter and receiver using Turbo coding [1]

6.6. Numerical Results

In this section, the performance of the proposed cooperative schemes is evaluated. Two types of scenarios are defined:

- The first scenario consists of four uniformly distributed single antenna UTs in a square with BSs in each of the corners. The power decay is proportional to $1/r^4$, where r is the distance from a transmitter. For this scenario the results are presented in terms of average BER as function of cell edge SNR defined as $\mathrm{SNR} = P_{t_b}\rho_c/N_C\sigma^2$ where ρ_c represents the long term channel power in the center of the square.
- In the second scenario we have four BSs, each equipped with four antennas, and four single antenna UTs. We assume the shadowing effects, modulated with a zero mean Gaussian variable and a variance of 6dB. For this scenario the results are presented in terms of average BER as function of per-BS SNR defined as $\mathrm{SNR} = P_{t_b}/N_C\sigma^2$.

The main parameters used in the simulation are based in the LTE standard [50]:

Table 4 - LTE-based simulation parameters

FFT size	1024
Available subcarriers (N_C)	128
Sampling Frequency	15.36 MHz
Useful Symbol Duration	66.6 µs
Cyclic Prefix Duration	5.21µs
Overall OFDM symbol duration	71.86µs
Subcarrier Separation	15kHZ
Modulation	QSPK
Channel Code	Uncoded / $^1/_2$ CTC (1536,3072)

The channel used was the LTE extended, with modified taps delays according to the sampling frequency defined by LTE standards.

Firstly, we analyze the performance of the precoder vectors with equal power allocation (EPA). Then, the results of the same precoder vectors with the discussed power allocation strategy are presented.

From the figure bellow, we can see that the implemented DVSINR precoder outperforms the DZF one. This is because the DVSINR is more efficient to remove the interference that the DZF, since it relax the orthogonality constraint required by the ZF. From the figure we can observe a gain about 5dB of the DVSINR against the DZF for a BER=10-3.

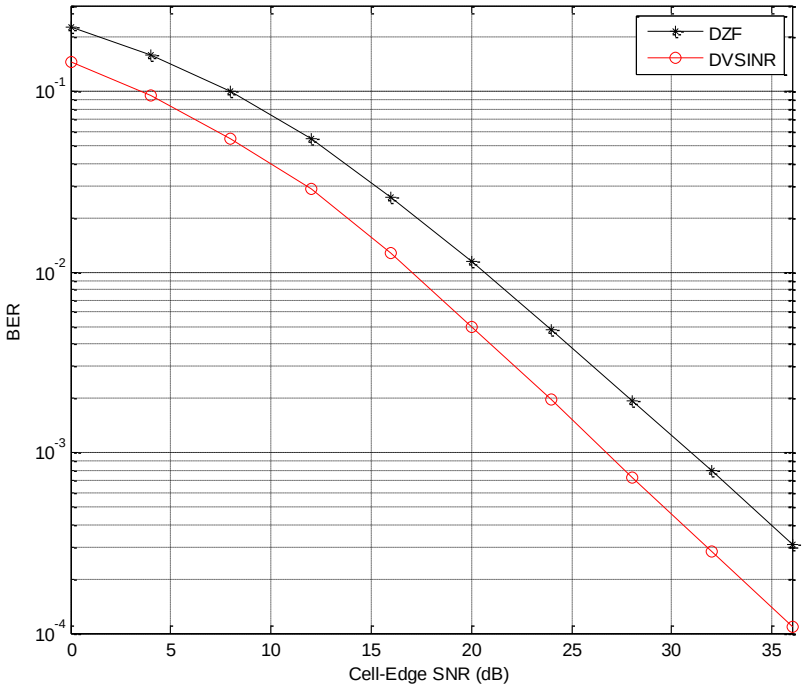

Figure 35 - Performance evaluation of the distributed precoding schemes for N_{tb}=4

If we add more antennas to each BS, the obtained results are shown in the figure bellow. In this scenario, the number of antennas per BS increases to 6 and the DoF (Degrees of Freedom) of the equivalent channel variables, given by $2(N_{t_b} - K + 1)$, increases from 2 (first scenario) to 6.

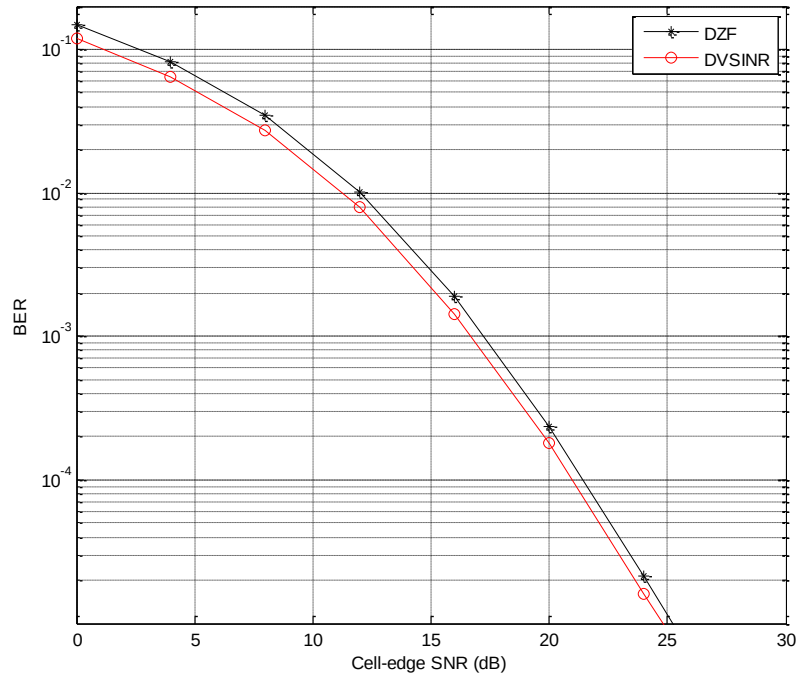

Figure 36 - Performance evaluation of the distributed precoding schemes for N_{tb} = 6

As we can observe, as we increase the DoF, the DZF tends to the DVSINR. This behavior is similar to the single cell systems where the precoders based on ZF criterion tend to the ones based on MMSE, as the number of transmit antennas(or DoF) increases, or at high SNR.

In Figure 37 we can perceive the effects of the previously defined power allocation scheme on the performance of the precoder vectors.

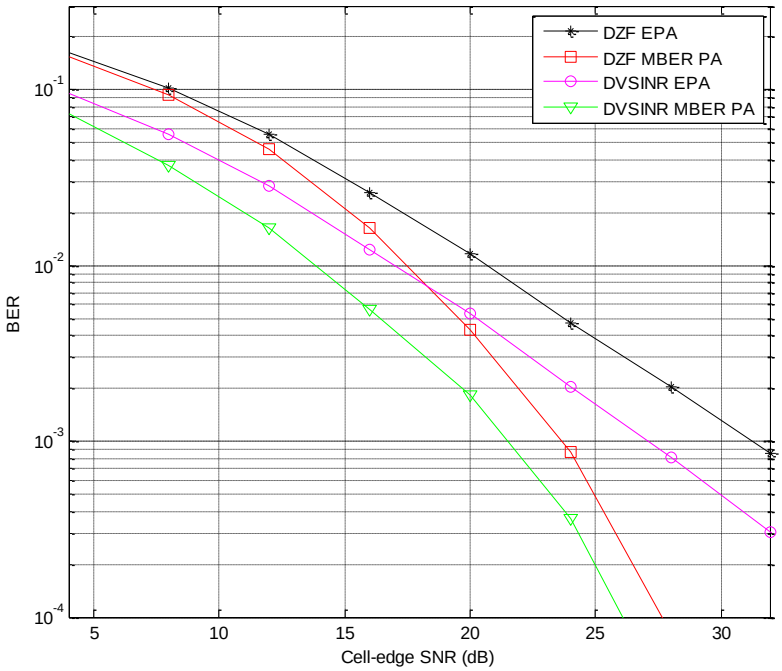

Figure 37 - Performance evaluation of the distributed precoding schemes with power allocation

From the figure above we can easily see that the performance of the distributed power allocation schemes outperform their equal power counterparts. This is due to the efficient redistribution of power across the different subchannels. As seen previous, the performance of the DZF MVBER PA tends to the DVSINR MBER PA for high SNRs.

Next we evaluate the performance of the pre-established system, used in the previous simulations, consisting of the distributed precoder vectors with power allocation strategies, when we add a coding block, which codifies that data using Turbo Coding. The block size used was of 1536, with a frame length of 12 OFDM symbols and a code rate of $1/2$.

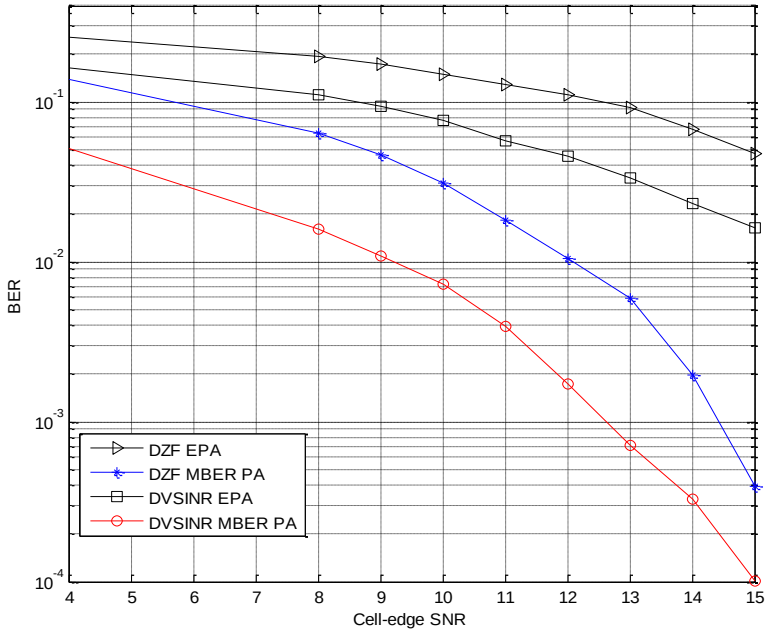

Figure 38 - Performance evaluation of the distributed precoder with power allocation with turbo coding

As we expected, the BER performance of the system improves significantly, especially for the precoder vectors with power allocation strategies. Although we are decreasing the number of errors in the system, we are diminishing its throughput, seen that we are sending less information bits.

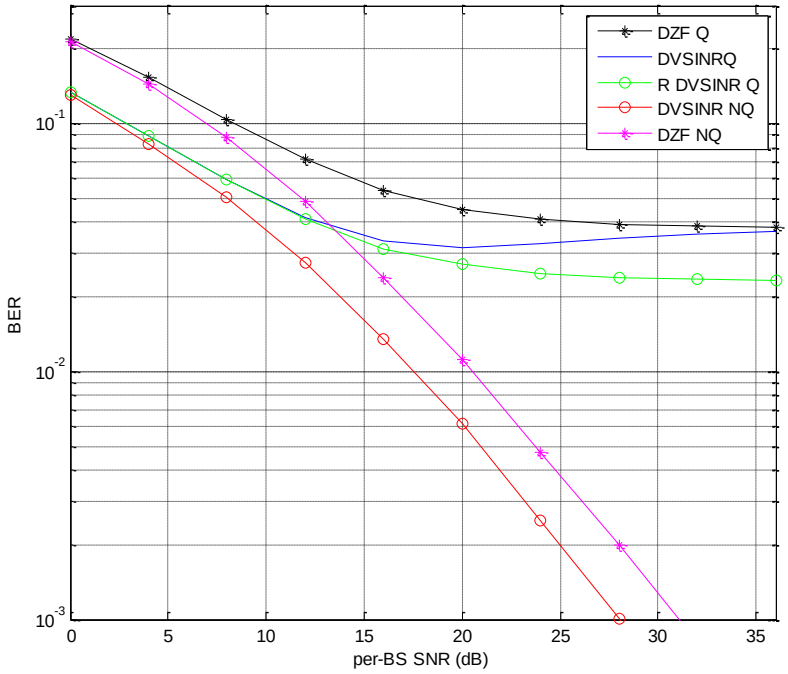

Figure 39 - Performance evaluation of channel quantization for m=4bits

Finally, we analyze the performance of the quantization process, for different amounts of quantization bits, more specifically, 4, 6 and 8 bits. These results were obtained by assuming equal power allocation. We now consider the second scenario, previously defined.

As can be seen by Figure 39, using 4 channel quantization bits, the performance is degraded mainly for high SNR regime. For low SNRs values, the performance is similar to the one obtained for the non-quantization scenario. Also, we can see that the proposed Robust-DVSINR (R-DVSINR) outperforms its counterparts mainly for high SNR regime. This is because now the precoder was designed to explicitly take into account the errors introduced by the channel. Using such a low amount of bits to quantize the CSI exchanged between BS may relieve the backhaul network but it degrades the performance of the cooperative techniques, allowing a very high number of errors in the system.

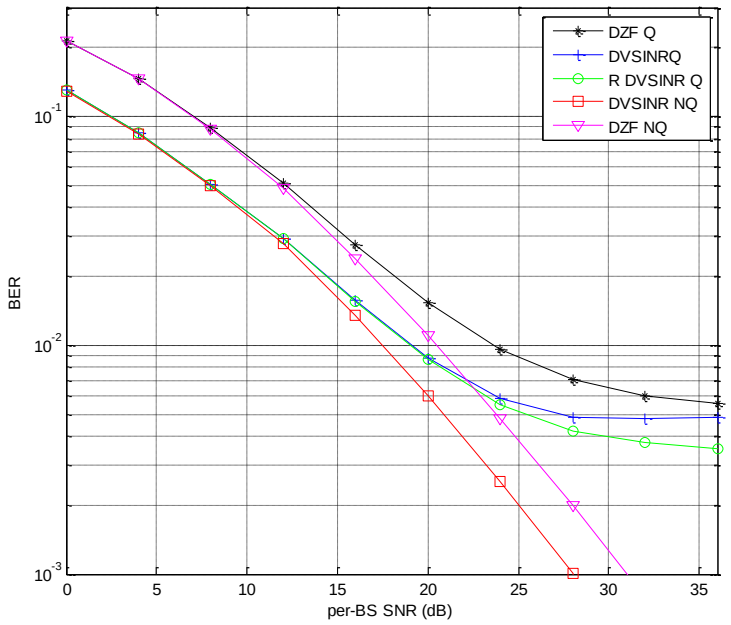

Figure 40 - Performance evaluation for channel quantization using m=6 bits

Increasing the number of channel quantization bits to 6, it is easy to see from the above figure that the BER performance improves substantially when compared to the previous approach, where 4 bits were used. In this case, the BER performance of the quantized approach is equal to the non-quantized one for low SNRs, starts degrading for medium SNRs and only for high SNRs presents bad BER results. As seen previously, the R-DVSINR approach is the one with better performance.

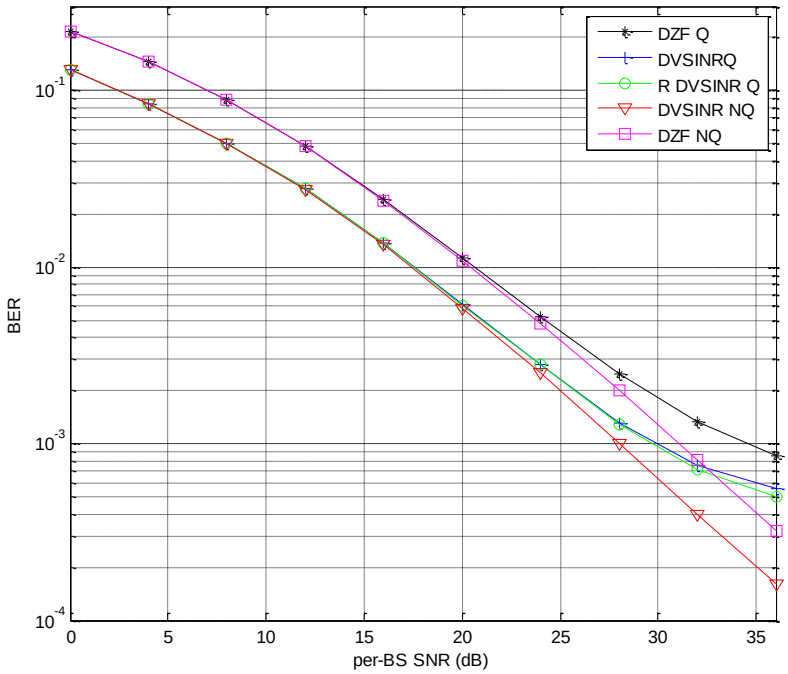

Figure 41 - Performance evaluation of channel quantization using m=8 bits

Finally, using 8 bits, we get results very similar to the ones without quantization, with only some discrepancies for very high SNR, in the order of 32 dB. With this amount of quantization bits, the performance of the R-DVSINR is not very different from the DVSINR. This is because the quantization error variance tends to zero when the number of bits increases and thus the R-DVSINR tends to the performance of the DVSINR.

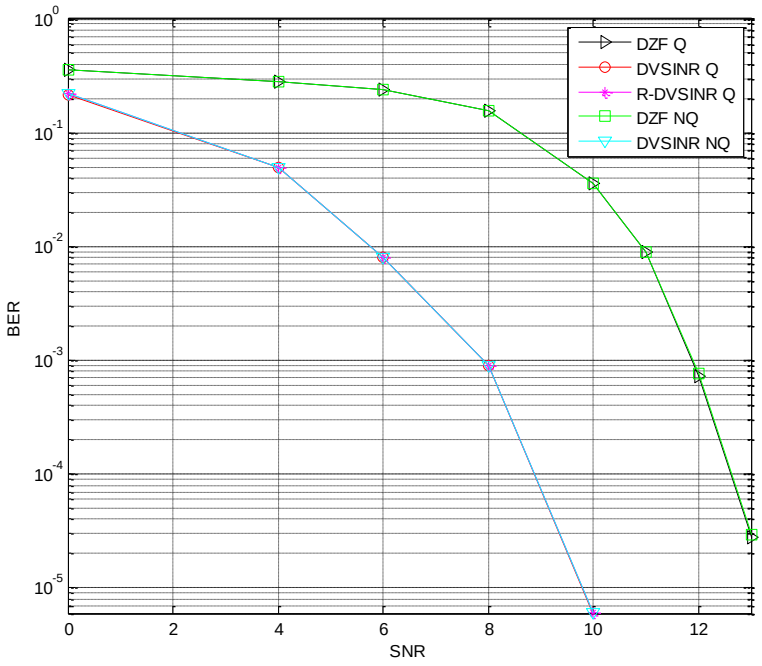

Figure 42 - Performance evaluation of the coded quantized schemes, using m=8 bits

Figures 42 and 43 present the results for the same previous quantized based schemes but now using the channel turbo codes, for m=8 and 4 , respectively.

From the results we can see that the channel turbo coding clearly outperforms the previous uncoded data scenarios. The results obtained when using 8 quantization bits, are nearly perfect, that is, the results are basically the same that the ones obtained with perfect CSI, even for high SNR regime.

As it was seen previously, the DVSINR approach outperforms the DZF one. The R-DVSINR is nearly identical to its counterpart that doesn't take in consideration the quantization noise. We can then conclude that coding helps to reduce the quantization noise.

.

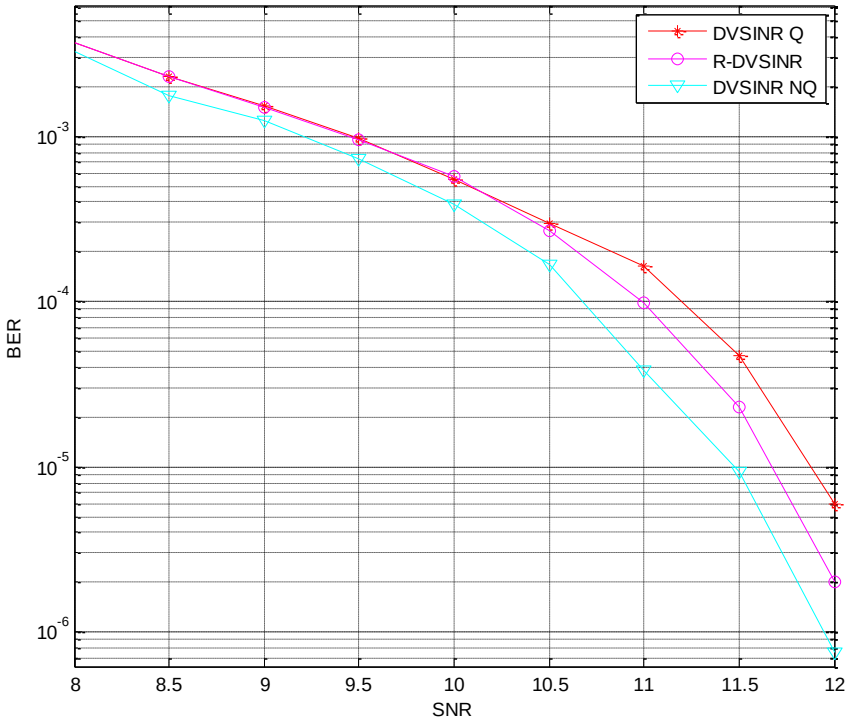

Figure 43 - Performance evaluation of the coded quantized schemes, with m=4 bits

For the case where we only use 4 bits for the CSI quantization, we only analyze the performance of the DVSINR and R-DVSINR approaches, seen that those clearly outperform the DZF ones, and thus we can better visualize the performance of the firstly stated approaches.

It is visible that for low SNRs, the quantized approaches have a performance very similar to the non-quantized one. This changes for medium valued SNRs, and from approximately 10dB we can see that the R-DVSINR starts outperforming DVSINR. Using 4 quantization bits, it is expected that the quantized schemes are outperformed by the non-quantized ones, but the R-DVSINR approach has a good performance, being the difference between the two approaches of approximately 0,5dB for a fixed BER of 10^{-4} .

7. Conclusions

Throughout this thesis, we studied the evolution of cellular communication systems and its constant progress to adjust to the exponential increasing number of users and new services. In order to support this growth, new techniques and technologies were implemented along the years, and it is the major advances in these technologies that demark the so called cellular systems generations. If in the first generation, the system was characterized by using analogue voice communications, the second generation was characterized by using digital voice communications. In third generation systems, the multimedia data services paradigm became a reality and now, with the introduction of the 4G concept, cellular systems gained higher data rates, better cell coverage and high mobility for the end user. Nevertheless, LTE still falls short, taking into account the actual data rate demands, and in order to correct that, LTE-Advanced is being developed.

After the quick overview of the cellular systems evolution, made in the first chapter of this thesis, we presented the major enabling technologies of LTE. First we introduced the Orthogonal Frequency Division Multiplexing (OFDM) concept and the multiple access technology OFDMA, which plays a major role in 4G and above systems. Afterwards, we introduced, in chapter 3 multiple antennas techniques, and the importance of MIMO systems to improve data rates, referring some of the foremost important concepts, such as spatial multiplexing and diversity.

Following the introduction of its enabling technologies in the previous chapters, we finally introduce the LTE system, presenting its major features, such as the network architecture and most importantly, the physical layer. Afterwards, we were in conditions to present the evolution of LTE, LTE-Advanced. In that chapter we presented some of the most important enabling technologies of LTE-Advanced. One of those technologies, and the focus of this thesis, is a concept named Coordinated Multipoint (CoMP). The main classes of CoMP were described, namely Joint Transmission and Coordinated Scheduling/Beamforming. Some attention was also given to some main concerns of a CoMP system, mainly the backhaul network and the clustering capacity.

In Chapter 6, we implemented several CoMP techniques. The core of these schemes is the use of distributed precoder vectors, with the intended of mitigating interference for cell-edge users. These distributed precoding vectors, DZF and DVSINR, implemented for the downlink of a MISO-OFDM system, were computed at each base station just by assuming the knowledge of local CSI, without data sharing. We concluded that the DVSINR precoder outperforms the DZF one. These results are not so evident when we increase the systems DoF, which causes the DZF approach to approximate the DVSINR one.

This scheme was further optimized with the use of distributed power allocation schemes, which clearly outperform the Equal Power ones. These power allocations schemes, as what

happened previously with the precoder vectors, are computed at each base station, in a distributed manner, assuming only the knowledge of the local CSI. Later we introduced channel coding to our system, introducing redundancy, thus reducing the probability of errors.

Finally, and with the intended of assessing the performance of the precoders under imperfect CSI, we introduced quantization techniques, where the CSI associated to the different links between the BS and the UT is feedback from the UT to the BS, and then exchanged by the different BSs. This information is then used to calculate the precoder vectors used previously but now with quantized CSI, for different amount of quantization bits. A new version of the DVSINR precoder that considered the quantization error, R-DVSINR, was considered. It was visible that the R-DVSINR outperformed the rest of the precoders, and that their performance deteriorates when the number of quantization bits decreases.

It is then clear that the presented techniques greatly improve the performance of cellular systems, and can be expected be featured in LTE-Advanced.

7.1. Future Work

For future work references, one would suggest:

- Extending the analyses made throughout this thesis to the uplink, but in this case efficient equalizers should be designed instead
- Comparing the performance of the analysed techniques with techniques that assume that the users' data is shared among the BSs, i.e., joint processing techniques.
- Extend the analyses for other more complex scenarios;
- Test these techniques in real life large-scale networks, using field trials in urban areas.

8. References

1. mobiThinking. *Global mobile statistics 2012 Home*. 2013 December 2012 [cited 2013 09/05/2013]; Available from: http://mobithinking.com/mobile-marketing-tools/latest-mobile-stats/.
2. Cox, C., *An Introduction to LTE: LTE, LTE-Advanced, SAE and 4G Mobile Communications*2012: Wiley.
3. Khan, F., *LTE for 4G Mobile Broadband: Air Interface Technologies and Performance*2009: Cambridge University Press. 506.
4. Technologies, A., *LTE and the Evolution to 4G Wireless: Design and Measurement Challenges*2009: John Wiley & Sons.
5. Edt, G., *Mobile WiMAX -- Part I: A Technical Overview and Performance Evaluation*2006.
6. Carew, S. *Qualcomm halts UMB project, sees no major job cuts*. 2013 13/11/2008 [cited 2013 09/05/2013]; Available from: http://www.reuters.com/article/2008/11/13/qualcomm-umb-idUSN1335969420081113?rpc=401&.
7. Americas, G. 2013 11/07/2013]; Available from: http://www.4gamericas.org.
8. Holma, D.H. and D.A. Toskala, *LTE for UMTS - OFDMA and SC-FDMA Based Radio Access*2009: Wiley Publishing. 450.
9. Tse, D. and P. Viswanath, *Fundamentals of Wireless Communication*2005: Cambridge University Press.
10. 3GPP, *3GPP RAN WG1 TR 25.814 v7.1.0, Physical Layer Aspects for Evolved UTRA (Release 7)*, 2006.
11. G. J. Foschini, M.J.G., *On Limits of Wireless Communications in a Fading Environment When Using Multiple Antennas.* Wireless Personal Communications, 1998. **Vol. 6**: p. 311–335.
12. 36.101, G.T., *User Equipment (UE) Radio Transmission and Reception*, in *section 7.2.*2011.
13. Alamouti, S. *Space block coding: A simple transmitter diversity technique for wireless communications*. IEEE Journal on Selected Areas in Communications, 1998.
14. Jankiraman, M., *Space-Time Codes and MIMO Systems with CDROM*2004: ARTECH HOUSE Incorporated.
15. 3GPP, *Requirements for Evolved Universal Terrestrial Radio Access (UTRA) and Universal Terrestrial Radio Access Network (UTRAN)*, in *TR 25.913*.

16. TeliaSonera. *Pioneering 4G networks*. [cited 2013 10/05/2013]; Available from: http://www.teliasonera.com/en/innovation/access-is-king/2011/4/pioneering-4g-networks/.

17. 3GPP, *Evolved Universal Terrestrial Radio Access Network (E-UTRA): Overall Description*, in *TS 36.300*.

18. Ghosh, A., et al., *LTE-advanced: next-generation wireless broadband technology [Invited Paper].* Wireless Communications, IEEE, 2010. **17**(3): p. 10-22.

19. Rezaei, F., M. Hempel, and H. Sharif. *LTE PHY performance analysis under 3GPP standards parameters*. in *Computer Aided Modeling and Design of Communication Links and Networks (CAMAD), 2011 IEEE 16th International Workshop on*. 2011.

20. Dabbagh, A.D., R. Ratasuk, and A. Ghosh. *On UMTS-LTE Physical Uplink Shared and Control Channels*. in *Vehicular Technology Conference, 2008. VTC 2008-Fall. IEEE 68th*. 2008.

21. Abdullah, M.F.L. and A.Z. Yonis. *Performance of LTE Release 8 and Release 10 in wireless communications*. in *Cyber Security, Cyber Warfare and Digital Forensic (CyberSec), 2012 International Conference on*. 2012.

22. Gesbert, D., et al., *Multi-Cell MIMO Cooperative Networks: A New Look at Interference.* Selected Areas in Communications, IEEE Journal on, 2010. **28**(9): p. 1380-1408.

23. Irmer, R., et al., *Coordinated multipoint: Concepts, performance, and field trial results.* Communications Magazine, IEEE, 2011. **49**(2): p. 102-111.

24. McCoy, W., *Overview of 3GPP LTE Physical Layer: White Paper by Dr. Wes McCoy.* 2007.

25. Young-Han, N., et al. *Cooperative communication technologies for LTE-advanced*. in *Acoustics Speech and Signal Processing (ICASSP), 2010 IEEE International Conference on*. 2010.

26. Ming Ding, H.L., *Multi-point Cooperative Communication Systems: Theory and Applications*2013: Shanghai Jiao Tong University Press.

27. Binbin, W., L. Bingbing, and L. Mingqian. *A Novel Precoding Method for Joint Processing in CoMP*. in *Network Computing and Information Security (NCIS), 2011 International Conference on*. 2011.

28. Sawahashi, M., et al., *Coordinated multipoint transmission/reception techniques for LTE-advanced [Coordinated and Distributed MIMO].* Wireless Communications, IEEE, 2010. **17**(3): p. 26-34.

29. Botella, C., et al. *On the Performance of Joint Processing Schemes over the Cluster Area*. in *Vehicular Technology Conference (VTC 2010-Spring), 2010 IEEE 71st*. 2010.

30. Rashid-Farrokhi, F., L. Tassiulas, and K.J.R. Liu, *Joint optimal power control and beamforming in wireless networks using antenna arrays.* Communications, IEEE Transactions on, 1998. **46**(10): p. 1313-1324.

31. Daewon, L., et al., *Coordinated multipoint transmission and reception in LTE-advanced: deployment scenarios and operational challenges.* Communications Magazine, IEEE, 2012. **50**(2): p. 148-155.

32. Marsch, P. and G. Fettweis. *A Decentralized Optimization Approach to Backhaul-Constrained Distributed Antenna Systems*. in *Mobile and Wireless Communications Summit, 2007. 16th IST*. 2007.

33. Papadogiannis, A., D. Gesbert, and E. Hardouin. *A Dynamic Clustering Approach in Wireless Networks with Multi-Cell Cooperative Processing*. in *Communications, 2008. ICC '08. IEEE International Conference on*. 2008.

34. A. G. Armada, M.S.F., and R. Corvaja, *Waterfilling schemes for zero-forcing coordinated base station transmissions.* proc. of IEEE GLOBECOM, 2009.

35. Jun, Z., et al., *Networked MIMO with clustered linear precoding.* Wireless Communications, IEEE Transactions on, 2009. **8**(4): p. 1910-1921.

36. Rui, Z. *Cooperative Multi-Cell Block Diagonalization with Per-Base-Station Power Constraints*. in *Wireless Communications and Networking Conference (WCNC), 2010 IEEE*. 2010.

37. Bjornson, E., et al., *Cooperative Multicell Precoding: Rate Region Characterization and Distributed Strategies With Instantaneous and Statistical CSI.* Signal Processing, IEEE Transactions on, 2010. **58**(8): p. 4298-4310.

38. A. Silva, R. Holakouei, and A. Gameiro, *Power allocation strategies for distributed precoded multicell based systems.* EURASIP Journal on Wireless Communications and Networking, 2011. **2011**(1): p. 1-1.

39. Lindblom, J., E. Karipidis, and E.G. Larsson, *Selfishness and altruism on the MISO interference channel: the case of partial transmitter CSI.* Communications Letters, IEEE, 2009. **13**(9): p. 667-669.

40. Jun, Z. and J.G. Andrews, *Adaptive Spatial Intercell Interference Cancellation in Multicell Wireless Networks.* Selected Areas in Communications, IEEE Journal on, 2010. **28**(9): p. 1455-1468.

41. Byong Ok, L., et al., *A novel uplink MIMO transmission scheme in a multicell environment.* Wireless Communications, IEEE Transactions on, 2009. **8**(10): p. 4981-4987.

42. R. Zakhour, D.G., *Coordination on the MISO Interference Channel using the Virtual SINR Framework*, in *International ITG/IEEE Workshop on Smart Antennas (WSA'09)*2009: Berlin, Germany.

43. S. Teodoro, A.Silva, R. Dinis, and A. Gameiro, *MMSE Interference Alignment Algorithms with Low Bit Rate Feedback*, in *Wireless Global Summit*2013: Atlantic City, USA.

44. José Assunção, R. Holakouei, A. Silva, Atílio Gameiro, *Performance Evaluation of Multicell Coordinated Beamforming Approaches for OFDM Systems*, in *Proc IARIA-International Conf. on Wireless and Mobile Communications - ICWMC*2012: Venice , Italy.

45. Haykin, S., *Adaptive filter theory (3rd ed.)*1996: Prentice-Hall, Inc. 989.

46. R. M. Corless, G.H.G., D. E. G. Hare, D. J. Jeffrey, D. E. Knuth, *On the Lambert W Function*. Adv. Comput. Math. Vol. 5. 1996: University of Waterloo, Computer Science Department.

47. ETSI, *LTE; Evolved Universal Terrestrial Radio Access (E-UTRA); Multiplexing and channel coding (3GPP TS 36.212 version 9.2.0 Release 9).* 2010.

48. Zarei, S. *Channel Coding and Link Adaptation*. 2009.

49. Berrou, C., A. Glavieux, and P. Thitimajshima. *Near Shannon limit error-correcting coding and decoding: Turbo-codes. 1*. in *Communications, 1993. ICC '93 Geneva. Technical Program, Conference Record, IEEE International Conference on*. 1993.

50. 3GPP, *LTE Physical Layer - General Description*, 2007.